Macromolecules
PERSPECTIVE

Macromolecules **2009**, *42*, 9369–9383 **9369**
DOI: 10.1021/ma902042x

Mixed Polymer Brush-Grafted Particles: A New Class of Environmentally Responsive Nanostructured Materials

Bin Zhao*,† and Lei Zhu‡

†*Department of Chemistry, University of Tennessee, Knoxville, Tennessee 37996, and* ‡*Department of Macromolecular Science and Engineering, Case Western Reserve University, Cleveland, Ohio 44106*

Received September 13, 2009; Revised Manuscript Received November 4, 2009

ABSTRACT: Mixed polymer brush-grafted particles, in which two distinct polymers are randomly or alternately immobilized by one end via a covalent bond on the surface of core particles with sufficiently high grafting densities, represent a new, intriguing class of environmentally responsive nanostructured hybrid materials. The two end-tethered polymers can undergo spontaneous chain reorganization in response to environmental variations, rendering particles adaptive surface properties and different colloidal behavior. This Perspective is intended to review recent exciting progress on the synthesis, responsive properties, self-assembled structures, and applications of mixed brush-grafted particles with a spherical core radius R_{core} significantly larger than, comparable to, and smaller than the root-mean-square end-to-end distances ($\langle R_{rms} \rangle$) of grafted polymers. The critical yet unsolved issues in the phase morphology of mixed homopolymer brushes and the hierarchical self-assembly of mixed brush-grafted particles are discussed.

Polymer Brush-Grafted Particles: Hairy Particles

Hairy particles are composed of a core and a layer of polymer chains that are densely tethered by one end via a covalent bond on the core surface (i.e., a polymer brush[1]).[2] The core can be an inorganic (e.g., silica),[2] a metal (e.g., gold),[3] or an organic (e.g., latex) particle[4] with a size from a few nanometers to hundreds of nanometers. Besides regular spherical shapes,[2−4] the core can also be cylindrical or rod-like.[5] The brush layer may be made of a neutral or a charged polymer, a flexible or a rigid-rod-like polymer, and a single-component or a multicomponent polymer system. Thus, the term "polymer brush-grafted particles" or "hairy particles" comprises a very broad range of nanostructured hybrid particles. These particles can be engineered to combine desired properties of both core particles (mechanical, optical,[6] magnetic,[7] etc.) and polymer brushes (environmental compatibility, responsiveness, etc.)[1,8] and thus have potential applications in diverse fields ranging from advanced nanocomposites,[2d] to catalysis,[2e,4c] to Pickering emulsions,[9,10] to self-cleaning materials,[10] to sensing,[11] and biotechnology.[12]

Generally, there are two approaches to prepare polymer brush-grafted particles: (i) the "grafting to" method, where end-functionalized polymers are grafted onto the surface of existing particles via a reaction between the polymer end group and the particle surface or act as a stabilizing reagent in the synthesis of core particles,[1b,12,13] and (ii) the "grafting from" method, where the tethered polymer chains are grown directly from initiator-functionalized particles.[1b,c,2] These two methods are complementary to each other, and each has distinct advantages. The "grafting to" method is simple in practice, and one can use well-defined polymers with known molecular architectures, predetermined molecular weights, and narrow polydispersities, but the grafting density of polymer brushes tends to be low because polymer chains must diffuse through the existing grafted polymer layer to react with the surface. The "grafting from" or surface-initiated polymerization method usually produces polymer brushes with a higher grafting density and a greater thickness, but it requires the immobilization of an initiator on the surface first.[1b,c,2,14]

The past decade has seen a rapid growth in the research of hairy particles. Since Prucker and Rühe described in their seminal papers the growth of polystyrene (PS) from silica gels that were functionalized with an azo monolayer by conventional free radical polymerizaiton,[2a,2b] a variety of polymerization techniques, particularly "living"/controlled radical polymerizations including atom transfer radical (ATRP),[15] nitroxide-mediated radical (NMRP),[16] and reversible addition−fragmentation chain transfer polymerization (RAFT),[17] have been used to synthesize high-density polymer brushes from silica particles,[2,18] gold and magnetic nanoparticles,[3,7] quantum dots,[6] and carbon nanotubes.[19] The availability of well-defined hairy particles with precisely determined structures in both core and brushes opens up new opportunities in fundamental studies and nano- and biotechnologies. For example, using the Langmuir−Blodgett technique, Ohno et al. demonstrated that the distance between the gold nanoparticles with a size of ∼10 nm can be well controlled by the chain length of the grafted polymer.[3a] They also discovered that under appropriate conditions high-density polymer brush-grafted silica particles can form semisoft colloidal crystals,[18h−j] a new type of colloidal crystals. Hairy particles have also been used for the fabrication of hollow organic particles[18e,k] and advanced polymer nanocomposites.[20] Magnetic nanoparticles grafted with biocompatible polymer brushes can be used as magnetic resonance imaging contrast agents.[12] By incorporating organic catalysts into dangling polymer chains grafted on particles, Zhao et al. developed polymer brush-supported catalysts that exhibit the advantages of both soluble polymer-supported (high catalytic activities) and cross-linked polymer-supported organocatalysts (high recyclability).[2e,4c] These examples demonstrate the unique characteristics of hairy particles compared with bare particles or small molecule-coated particles.

Among all types of polymer brush-grafted particles, environmentally responsive hairy particles are particularly interesting as they exhibit different structures and properties in response to

*Corresponding author. E-mail: zhao@ion.chem.utk.edu.

Published on Web 11/19/2009

environmental variations.[2e,13,21−23] These particles are usually made by the use of stimuli-responsive polymers, the polymers that exhibit an abrupt change in chain conformations upon application of an external stimulus (e.g., a temperature change, light, etc.).[24] A representative example of such polymers is thermosensitive hydrophilic polymers that can undergo coil-to-globule or hydration-to-dehydration transitions in water at lower critical solution temperatures (LCSTs).[25] Since the polymer brushes dictate how hairy particles interact with environment, the conformation changes of individual polymer chains could cause the particles to exhibit different behaviors. For example, thermosensitive polymer brush-grafted silica particles can spontaneously transfer from water to ethyl acetate phase upon heating or vice versa upon cooling.[22b] The thermo-induced transport of hairy particles is fully reversible and quantitative, which could be used to design novel phase transfer catalysts or material-delivery systems.

A new type of environmentally responsive hairy particles that has received growing interest in recent years is mixed brush-grafted particles,[26] in which two distinct, immiscible polymers are randomly or alternately immobilized by one end via a covalent bond with sufficiently high grafting densities on the surface of core particles. Unlike conventional stimuli-responsive, e.g., thermosensitive, hairy particles where individual polymer chains exhibit different chain structures and properties upon application of an external stimulus, the responsive properties of mixed brush-grafted particles stem from the capability of two immiscible components to undergo structural reorganization in a confined geometry in response to environmental variations in order to achieve the lowest free energy states. Thus, the two grafted polymers are not necessarily stimuli-responsive as in the conventional definition. Certainly, the use of stimuli-responsive polymers in the design and synthesis of mixed brush-grafted particles would further enrich their phase behavior and responsive properties. Before we consider mixed polymer brush-grafted particles, it would be beneficial to briefly discuss mixed homopolymer brushes in general.

Mixed Homopolymer Brushes on Planar Solid Substrates: Theoretical and Simulation Studies

Much like diblock copolymers, when molecular weights are sufficiently high, the two immiscible homopolymers in mixed brushes will undergo microphase separation; the covalent fixation of one end of polymer chains on a solid surface prevents macroscopic phase segregation.[27−29] The phase behavior of binary mixed homopolymer brushes on a planar solid substrate is dictated by a number of factors, including (i) degree of polymerization (DP) of each grafted polymer (N_A and N_B), (ii) Flory−Huggins interaction parameters between two components (χ_{A-B}), between each polymer and environment (χ_{A-E} and χ_{B-E}), and between each polymer and the grafting substrate (χ_{A-S} and χ_{B-S}), where A, B, E, and S represent respectively polymer A, polymer B, environment E (E could be a solvent or a polymer matrix, etc.), and substrate, (iii) grafting density of each polymer, and (iv) distribution of grafting sites of two polymers on the substrate. Although diblock copolymers and mixed homopolymer brushes have many characteristics in common (one extreme case of mixed homopolymer brushes is Y-shaped brushes made by grafting a diblock copolymer through the junction point to the surface), one distinct difference is that the junction points of block copolymer chains are mobile at the interface of different microdomains, while the grafting sites of two homopolymers in the mixed brushes are fixed.[30] In addition, mixed brushes are just a single brush layer with a typical thickness less than 100 nm. Thus, environmental factors could play a decisive role in the determination of phase structures of mixed brushes, making them exhibit different surface properties under different conditions. The distinctive

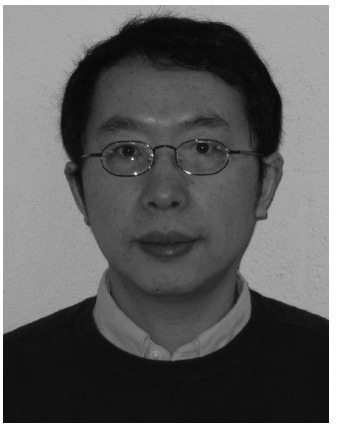

Bin Zhao is currently an Associate Professor of Chemistry at the University of Tennessee, Knoxville (UTK). He received his B.S. degree in 1992 and M.S. degree in 1995 both in polymer chemistry from the University of Science and Technology of China. In 1996, he came to the U.S. to pursue his Ph.D. degree in the Department of Polymer Science at the University of Akron, where he worked under Professor William J. Brittain. After finishing his dissertation defense in 2000, he joined Professor Jeffrey S. Moore's group at the University of Illinois at Urbana−Champaign as a postdoctoral researcher and worked on microfluidics. He started his independent career in the Department of Chemistry at UTK as an Assistant Professor in August 2002 and was promoted to Associate Professor with tenure in August 2008. His current research interests include environmentally responsive hairy particles, stimuli-sensitive block copolymer micelles and gels, and supported catalysts.

Lei Zhu is currently an Associate Professor of Macromolecular Science and Engineering at Case Western Reserve University. He received his B.S. degree in Materials Chemistry in 1993 and M.S. degree in Polymer Chemistry and Physics in 1996 from Fudan University. He earned his Ph.D. degree in Polymer Science in 2000 from the University of Akron, where he worked under the direction of Professor Stephen Z. D. Cheng. After two-year postdoctoral experience at University of Akron, he joined Institute of Materials Science and Department of Chemical, Materials and Biomolecular Engineering at University of Connecticut, as an Assistant Professor. In 2009, he moved to Case Western Reserve University. He is recipient of NSF Career Award, 3M Nontenured Faculty Award, and DuPont Young Professor Award. His research interests include polymer and polymer−inorganic hybrid materials for electric energy storage, development of artificial antibody as nanomedicines, and supramolecular self-assembly of discotic liquid crystals.

Scheme 1. A Simplified Schematic Illustration of Self-Assembly of Mixed Homopolymer Brushes under Equilibrium Melt Conditions and in Various Solvents

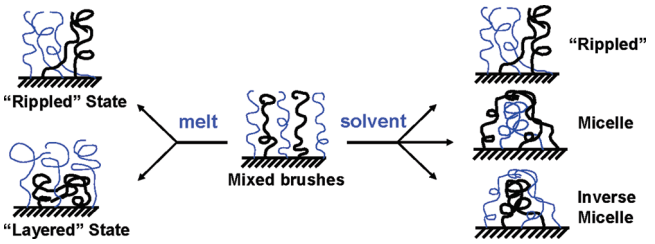

responsive properties and intriguing phase behavior of mixed brushes have attracted considerable interest and have been intensively studied by theoretical considerations and simulations in the past two decades.

Marko and Witten were the first studying whether symmetric mixed homopolymer brushes on a flat substrate phase separate laterally forming a "rippled" phase or vertically producing a "layered" structure under equilibrium melt conditions (Scheme 1).[27a,b] The lowering of enthalpy via microphase separation is accompanied by an entropic cost, which originates from the distribution of free ends within the layer in the case of vertical separation or the changes in the conformations of chains traveling in different regions of the brush layer in the case of lateral separation. They predicted that the lateral phase separation preempts vertical phase segregation and the "rippled" structure should be the one to appear. The phase separation is expected to occur at a molecular weight 2.27 times that for the same polymers in a simple blend at its demixing threshold, that is, $\chi_{AB}N = 4.54$, where N is the DP of one grafted polymer. The ripple wavelength of the pattern is predicted to be 1.97 times the chain root-mean-square end-to-end distance ($\langle R_{rms} \rangle$). Marko and Witten also pointed out that the phase transition can be controlled in a number of ways. For example, altering the relative compositions and molecular weights should drive first-order transitions between different ordered states. The lateral phase separation of mixed homopolymer brushes under melt or near-melt conditions has also been revealed by other researchers in theoretical or simulation studies.[27c,d,28c] Dong investigated the phase separation of mixed brushes in melt under a strong demixing interaction and found that in order to reduce the free energy the unlike chains undergo lateral microphase separation and form periodic pure A and B regimes, but it is unclear whether a striped pattern or a checkerboard pattern is preferred.[27c] The spatial period of the pattern is independent of the interaction strength between two polymers.[27c,28c] It should be noted here that in these studies it is implied that χ_{A-E} and χ_{B-E} are equal as well as the interaction strengths between two polymers and the grafting plane ($\chi_{A-S} = \chi_{B-S}$). If the surface free energy difference between two polymers is substantial, the species with a lower surface free energy may segregate in melt to the outermost layer to reduce the system's free energy. Similarly, the polymer with a lower interfacial free energy with respect to the grafting plane may have a stronger affinity to the substrate. However, no systematic theoretical investigations have yet been performed to elucidate the effects of the differences between χ_{A-E} and χ_{B-E} and between χ_{A-S} and χ_{B-S}.

In the presence of solvents, mixed homopolymer brushes exhibit an even richer phase behavior than in melt as the solvent quality can be readily tuned from nonselective good, to nonselective poor, and selective.[28,29] Many nanostructures have been predicted for planar mixed brushes in nonselective solvents. Lai studied binary mixed brushes in a good solvent by simulation and found that for symmetric binary brushes polymer chains of the same type clustered together laterally, forming a rippled state.[28a] For asymmetric mixed brushes, layered structures were observed with the minority chains being more stretched and staying away from the grafting sites under partial phase separation. The heights of both minority and majority chains in the layered state were proportional to their chain lengths. Soga et al. studied equilibrium structures of mixed brushes under various nonselective solvent conditions.[28b] When the two species are sufficiently immiscible, lateral microphase separation is observed over a wide range of solvent conditions. The onset of lateral phase separation is delayed as the solvent quality improves. Zhulina and Balazs designed an ideal binary mixed brush, Y-shaped brush in which a symmetric AB diblock copolymer is densely grafted on a substrate surface through a functional group at the junction point of the two blocks and studied how the variations of nonselective solvent quality, grafting density, and chain length affect the morphology of the Y-shaped brushes.[28c] A rich variety of lateral nanostructures within the brush layer was observed, and a phase diagram was constructed to delineate the regimes where different self-assembled nanostructures appear. Müller further investigated the structure and phase behavior of binary mixed brushes in nonselective solvents as a function of stretching, composition, and incompatibility of polymer chains.[28d] At small incompatibilities, a rippled phase is formed where different species segregate into an array of parallel cylinders. At large incompatibilities or asymmetric compositions, two "dimple" phases were identified, where different species form clusters that arrange on a quadratic (checkerboard structure) or hexagonal lattice. By using Monte Carlo simulations, Wenning et al. studied how the distribution of grafting points of two polymers influence the structure formation and found that the density fluctuation of grafting points enhances the formation of irregular structures and the randomness prevents the formation of a long-range order.[28f] The lack of a long-range periodic order in the nanostructures formed from microphase separation of binary mixed brushes was also observed in the studies using single-chain-in-mean-field simulations.[28g]

In selective solvents, micellar structures with the solvophobic chains packing into a dense core and the solvophilic chains forming the corona have been predicted.[29] Since the solvophilic chains are swollen in the solvents, the brush surface exhibits the properties of the solvophilic polymer. By varying the selective solvents, one can reversibly change the surface properties of mixed brushes. The switching process of binary mixed brushes composed of hydrophobic and hydrophilic species upon a sudden change of solvent quality was analyzed by Merlitz et al. for various solvent selectivities, chain lengths, and grafting densities.[29c,d] The process is highly reversible because after a microphase separation the chains are moving collectively inside their phase domains so that the interactions between chains of different types are diminished.

The above theoretical and simulation studies evidently show that by tuning parameters, including N_A and N_B, relative and overall grafting densities, chemical compositions, and solvents, a variety of surface nanostructures could be formed by binary mixed homopolymer brushes. Moreover, different structures formed from the same mixed brushes are fully reversible because polymer chains are covalently fixed on the substrate, making mixed brushes robust surface-responsive materials.[8]

Mixed Polymer Brushes on Planar Solid Substrates: Experimental Studies

Experimental study on mixed brushes began a decade ago.[31] Sidorenko et al. reported in 1999 the synthesis of first mixed homopolymer brushes, mixed PS/poly(2-vinylpyridine) (PVP) brushes, by a "grafting from" method using a two-step conventional free radical polymerization process, in which the second

Scheme 2. Synthesis of Mixed Homopolymer Brushes by Sequential Surface-Initiated Atom Transfer Radical Polymerization (ATRP) and Nitroxide-Mediated Radical Polymerization (NMRP) from Y-Initiator-Functionalized Silicon Wafers in a Two-Step Process (Adapted from Refs 63 and 64)

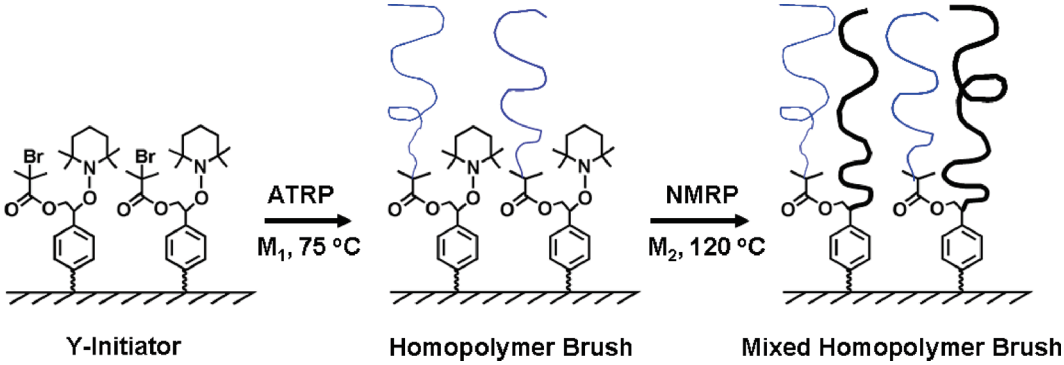

polymer was grown from the residual surface-immobilized azo initiator that did not decompose in the synthesis of the first polymer.[31] The obtained binary mixed brushes exhibited switching properties in response to environmental variations. Upon exposure to toluene, a selective solvent for PS, the surface became hydrophobic with PS chains occupying the outermost layer; treatment with an acidic aqueous solution, a selective solvent for PVP, changed the brush surface to hydrophilic due to the enrichment of PVP chains at the upper layer. These processes were reversible. Since this seminal experimental work, the intriguing responsive properties of mixed brushes have received enormous interest, and considerable efforts have been invested on the synthesis, characterization, phase morphologies, and applications of mixed brushes,[31−69] especially the mixed brushes on planar solid substrates in the past decade.

Besides the two-step surface-initiated conventional free radical polymerization,[31−42] various "grafting to" methods have also been developed for the preparation of mixed brushes. Notably, Minko et al. reported a "grafting to" method, in which carboxyl-terminated PS and PVP were grafted sequentially onto silicon wafers that were functionalized with 3-glycidoxypropyltrimethoxysilane at temperatures above the glass transition temperatures (T_gs) of polymers.[43,44] As mentioned earlier, the "grafting to" method allows the use of polymers with controlled molecular weights, narrow polydispersities, and well-defined architectures.[43−60] Wang et al. prepared mixed PS/poly(methyl methacrylate) (PMMA) brushes on silicon wafers by grafting ABC triblock copolymers with a short central B block that can form covalent bonds with silicon wafers in an one-step reaction.[57] The polymers used, PS-*b*-poly(4-hydroxystyrene)-*b*-PMMA and PS-*b*-poly(4-urethanopropyltriethoxysilylstyrene)-*b*-PMMA, were synthesized by living anionic polymerization and subsequent polymer modification reactions. Julthongpiput et al. prepared a Y-shaped brush, the model brush that Zhulina and Balazs studied in their theoretical work, by grafting PS-*b*-poly(*tert*-butyl acrylate) (P*t*BA) to silicon wafers via the reaction between the surface and the carboxylic acid group at the junction point of PS and P*t*BA blocks.[58,59] Similarly, Wang et al. synthesized Y-shaped PS/PVP brushes on silicon wafers via a hydrosilylation reaction.[60] A distinct advantage of Y-shaped brushes is that the fluctuation of grafting points of two polymers is completely eliminated, and two polymers are alternately grafted on the surface. However, the thickness of these Y-shaped brushes is low, typically < 5 nm.[57−60]

Zhao et al. developed a "grafting from" method for the synthesis of mixed homopolymer brushes with controlled molecular weights, narrow polydispersities, and high grafting densities by combining two different living radical polymerization techniques,[61−65] ATRP and NMRP, from asymmetric difunctional initiator- (Y-initiator-) functionalized silica wafers (Scheme 2).[63−65] The Y-initiators were designed to ensure that the ATRP and NMRP initiators are alternately immobilized on the substrate surface, and thus it is possible to prepare well-mixed homopolymer brushes. The NMRP initiator (TEMPO initiator) was confirmed to be stable under the typical ATRP conditions.[61−65,70] Corresponding free initiators were added into the reaction mixtures to control the surface-initiated polymerizations. The grafting densities of two polymers were high and very close to each other. The brush thickness was proportional to the polymer molecular weight, and a thickness of 76.5 nm was obtained for a mixed brush with a molecule weight of 36−40 kDa for each polymer.[63]

The responsive properties of mixed brushes upon environmental variations, including solvent changes and heating, have been intensively studied and well documented in the literature.[31−65] The changes in chemical composition of the topmost layer, topography, wettability, and mechanical properties have been investigated by contact angle analysis, X-ray photoelectron spectroscopy (XPS), atomic force microscopy (AFM topography and nanomechanical analysis), and ellipsometry. While most studies were performed ex-situ, e.g., on samples that were exposed to a solvent and subsequently dried with a stream of air or nitrogen, in-situ observations of the reorganization of mixed brushes in response to solvent changes were conducted by Lin et al. using AFM[66] and by Mikhaylova et al. using ellipsometry.[54] The wettability switching of amphiphilic mixed brushes can be amplified by surface roughness, which has been elegantly demonstrated by Minko et al. using a rough surface as the substrate to prepare mixed poly(styrene-*co*-2,3,4,5,6-pentafluorostyrene) (PSF)/PVP brushes.[46] The surface exhibited an advancing contact angle of 160° after exposure to toluene, and water could readily roll off. In contrast, water spread on the surface after the sample was treated with an acidic aqueous solution. The switching properties of mixed brushes have also been exploited in environmentally responsive lithography, where a pattern that was "written" in the mixed brushes by UV irradiation through a photomask can be reversibly developed and erased by treatments with different solvents.[47] Applications of binary mixed polymer brushes in microfluidic systems, chemical gating, and biotechnology have been reported.[67−69]

Understanding how two polymers organize themselves in the mixed brush layer under different conditions will increase our knowledge about polymer microphase separation in a confined geometry and allow better use of these surface-responsive materials in technological applications. Efforts have been made to elucidate the phase morphology of mixed brushes after exposure to different solvents. Minko et al. used AFM and X-ray photoemission microscopy to study mixed PSF/PMMA brushes, which were prepared by surface-initiated conventional free radical polymerizations from silicon wafers, and observed that in a nonselective solvent different species segregate into parallel cylinders ("ripple" structure).[28e] Upon exposure to a selective

solvent, the "ripple" structure transformed to a "dimple" structure, in which the unfavored component formed clusters, and simultaneously an enhanced perpendicular segregation was observed. In a separate work, they investigated the structure of mixed PS/PMMA brushes by a combination of step-by-step oxygen plasma etching and AFM ("AFM tomography").[38] The brushes exhibited ripple and dimple morphologies upon exposure to toluene, a nonselective solvent, and acetone, a selective solvent for PMMA, respectively. They concluded that the ripple morphology consisted of depressed PS-rich and elevated PMMA-rich elongated domains. For the dimple morphology, the core of the cluster was rich in PS, while the very top layer and valleys between clusters were rich in PMMA.

Although experimental studies had been performed to elucidate the nanostructures of mixed brushes after solvent treatments, the phase morphologies of mixed brushes had not been unequivocally determined; no direct visualization had been made, for example, by transmission electron microscopy (TEM) to show how the two polymers are organized in the brush layer. The phase behavior of symmetric mixed homopolymer brushes in melt, discussed by Marko and Witten,[27a] had not been touched. This is largely because of two challenges encountered in the experimental studies. One is the preparation of relatively well-defined mixed homopolymer brushes with controlled molecular weights, narrow polydispersities, and relatively high grafting densities. This requirement is similar to that for the study of phase morphology of block copolymers, where the samples used are well-defined and usually made by living polymerizations. The Y-brushes prepared from well-defined diblock copolymers by "grafting to" are truly alternate mixed brushes, but the thickness tends to be low, < 5 nm as reported in the literature.[57−60] The two-step surface azo-initiated radical polymerization can produce thick brushes, but the molecular weights and polydispersities are not controlled.[31−42] The second challenge is the experimental determination of phase structures. Although contact angle measurements, XPS, and AFM can give some insights, direct and explicit determination of phase behavior of mixed brushes requires the use of TEM, scattering methods, or differential scanning calorimetry (DSC), typical tools used in the study of block copolymers. The mixed brushes prepared by sequential surface-initiated ATRP and NMRP from a Y-initiator-functionalized substrate are relatively well-defined. However, microtoming of silicon wafers (e.g., by focused ion beams) for the preparation of TEM samples is very challenging.[71]

Mixed Brush-Grafted Particles: A New Intriguing Class of Environmentally Responsive Hairy Particles

Grafting two different polymers at the surface of particles in a random or alternate fashion with sufficiently high grafting densities for both polymers will produce a class of unprecedented hairy particles.[72] These hybrid particles undoubtedly possess environmentally responsive properties as mixed brushes on flat solid substrates, but they are not simply a curved version of planar mixed brushes for the following two reasons. First, interesting properties such as mechanical,[2] optical,[3,6,13] and magnetic properties,[7,12] which usually are not associated with polymers, can be introduced into hairy particles through the selection of appropriate core particles. Second, a new fundamental parameter, the curvature of the grafting surface, emerges, which could play an important role in the determination of phase structures of mixed brushes on particles. New nanostructures could be generated from microphase separation of mixed brushes when the core is small.

The effect of substrate curvature on phase morphology of mixed homopolymer brushes has largely remained unexplored. There is only one computer simulation study on mixed brushes

Scheme 3. Mixed Homopolymer Brushes Grafted on Spherical Particles with a Radius R (i) Significantly Larger than the Root-Mean-Square End-to-End Distances ($\langle R_{rms}\rangle$) of Polymers, (ii) Smaller than $\langle R_{rms}\rangle$, and (iii) Comparable to $\langle R_{rms}\rangle$

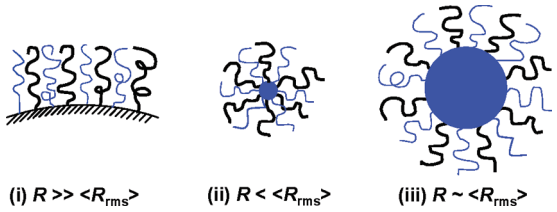

that are grafted on spherical particles with a core radius R comparable to the polymer size $\langle R_{rms}\rangle$.[73] The phase behaviors of mixed brushes on spherical particles of other sizes and particles of other shapes and sizes have not been investigated theoretically. There have been a number of experimental studies on spherical particles.[10,26,74−90] In the following sections, we will discuss, whenever applicable, the synthesis, responsive properties and phase morphologies of mixed brushes on spherical particles with a radius R (i) significantly larger than $\langle R_{rms}\rangle$ of polymers having the same molecular weights in an ideal state, (ii) smaller than $\langle R_{rms}\rangle$, and (iii) comparable to $\langle R_{rms}\rangle$ (Scheme 3). This classification is arbitrary, solely based on the authors' opinion. In doing so, the authors hope to convey a sense to readers that mixed brush-grafted particles are an intriguing class of nanostructured materials and are of great interest to both academic research and technological applications. Besides the morphologies of mixed brushes on the surface of particles, attention will also be paid to the hierarchical structures formed by self-assembly of hairy particles under various environmental conditions.

Mixed Brush-Grafted Particles with a Core Size Significantly Larger than Root-Mean-Square End-to-End Distances $\langle R_{rms}\rangle$ of Polymers

When the size of core particles is significantly larger than the $\langle R_{rms}\rangle$ of the polymers in an ideal state, mixed brushes can be considered to be grafted on a quasi-planar substrate. Compared with silicon wafers, the higher surface area of particles and the increased amount of grafted polymers allow the use of traditional block copolymer characterization techniques for study of phase behavior of mixed homopolymer brushes. These techniques include DSC, TEM, and neutron scattering, which have been routinely employed to determine phase morphologies of block copolymers in melt and in solution.[91,92] Different from silicon wafers, silica particles can be microtomed to thin sections for direct visualization by TEM. Moreover, the higher surface area of particles allows the cleavage of grafted polymers for thorough characterization of molecular weights, polydispersities, and grafting densities if mixed brushes are synthesized by surface-initiated polymerizations. These molecular characteristics are important for the study of phase behavior of mixed homopolymer brushes.

Aiming at determining the phase structures of mixed homopolymer brushes in melt and in solution, Zhao and co-workers synthesized mixed poly(*tert*-butyl acrylate) (P*t*BA)/PS brushes with controlled molecular weights and narrow polydispersities from Y-initiator-functionalized silica particles with a size of 180 nm by sequential ATRP of *tert*-butyl acrylate and NMRP of styrene in the presence of corresponding free initiators.[26] By cleaving the grafted polymers off the silica particles, the molecular weights and polydispersities of grafted polymers were found to be essentially identical to those of free polymers formed from free initiators in solutions. A significant portion of the polymer mixture cleaved from mixed P*t*BA/PS brush-grafted silica particles was the diblock copolymer, implying that the two

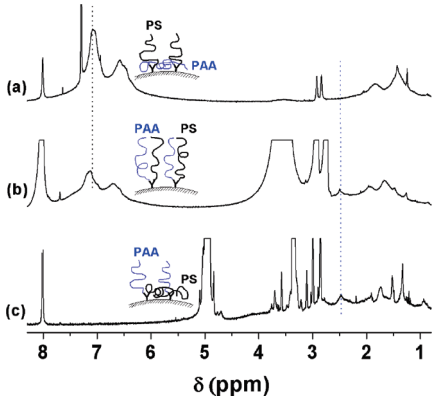

Figure 1. ^{1}H NMR spectra of mixed PAA/PS brush-grafted silica particles in (a) $CDCl_3$, (b) DMF-d_7, and (c) CD_3OD. A drop of DMF-d_7 was added into the particles prior to $CDCl_3$ and CD_3OD to facilitate the dispersion of hairy particles. Mixed PAA/PS brush-grafted particles were synthesized from P*t*BA/PS brush-grafted particles with P*t*BA M_n of 24.2 kDa and PS M_n of 23 kDa. The grafting densities of P*t*BA and PS were 2.5 and 2.7 nm^2/chain, respectively (reproduced and adapted from ref 26).

homopolymers were nearly alternately grafted on the surface of particles.[26] Thus, the local fluctuation of grafting points was largely eliminated, making the system well suited for phase morphology study.[93] Amphiphilic mixed poly(acrylic acid) (PAA)/PS brush-grafted particles were synthesized from mixed P*t*BA/PS brush-grafted particles by the removal of *tert*-butyl groups of P*t*BA. The calculated average distance between grafting sites was 1.1−1.2 nm. To confirm that the tethered polymers are in the brush regime, we estimated the radii of gyration ($\langle R_g \rangle$) of free polymers having the same molecular weights in their ideal states and found that they were more than twice larger than the average distance between the grafting points, suggesting that the grafted polymers were in the highly stretched brush regime.[94]

These hairy particles exhibited environmentally responsive properties. For example, amphiphilic mixed PAA/PS brush-grafted particles can be dispersed in chloroform, a selective solvent for PS, and methanol, a selective solvent for PAA, forming stable dispersions.[26] The capability of mixed brushes to undergo self-reorganization in response to environmental variations can be better seen from ^{1}H NMR spectroscopy analysis (Figure 1). For the hairy particles in DMF-d_7, a nonselective good solvent for both polymers, the peaks from both PAA and PS were visible, indicating that the two polymers were mobile. In $CDCl_3$, a selective solvent for PS, the grafted PAA chains collapsed, which was evidenced by the disappearance of the characteristic peak from PAA at ~2.5 ppm, while the signal from PS remained visible. In contrast, in CD_3OD, a selective solvent for PAA, the grafted PS collapsed, but the PAA chains were mobile.[26]

To determine whether symmetric mixed homopolymer brushes undergo lateral or vertical microphase separation in melt, we used DSC and TEM to investigate the mixed P*t*BA/PS brushes on silica particles.[74] DSC studies showed that for thermally annealed mixed P*t*BA/PS brushes with P*t*BA M_n of 24.2 kDa and PS M_n of 23.0 kDa (the high molecular weight (MW) sample) two glass transitions were observed at 44 and 90 °C, which corresponded to the T_gs of P*t*BA and PS, respectively, suggesting that the two grafted polymers phase-separated into microdomains that consisted of nearly pure polymers. In contrast, mixed P*t*BA/PS brushes with P*t*BA M_n of 10.4 kDa and PS M_n of 11.9 kDa (the low MW sample) exhibited only one broad glass transition with a middle point at 83 °C, implying that the two grafted polymers in this sample did not strongly phase separate. Figure 2 shows the typical TEM micrographs of microtomed thin sections

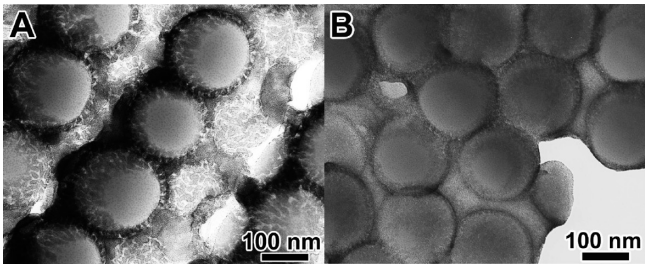

Figure 2. TEM micrographs of thin sections of (A) the thermally annealed high MW sample (mixed brushes with P*t*BA M_n of 24.2 kDa and grafting density of 2.5 nm^2/P*t*BA chain and PS M_n of 23.0 kDa and grafting density of 2.7 nm^2/PS chain) and (B) low MW sample (mixed brushes with P*t*BA M_n of 10.4 kDa and grafting density of 3.1 nm^2/P*t*BA chain and PS M_n of 11.9 kDa and grafting density of 2.9 nm^2/PS chain) after staining with RuO_4 for 30 min (reproduced from ref 74).

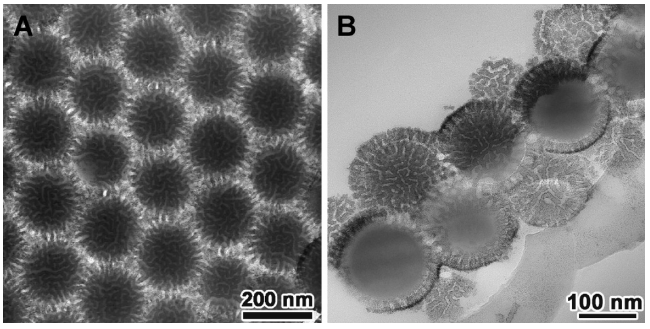

Figure 3. Bright field TEM micrographs of (A) a top view and (B) a cross-sectional view of a mixed brush sample with P*t*BA M_n of 24.2 kDa and grafting density of 2.5 nm^2/P*t*BA chain and PS M_n of 23.0 kDa and grafting density of 2.7 nm^2/PS chain that was cast from $CHCl_3$, a good solvent for both P*t*BA and PS. The samples were stained with RuO_4 vapor for 30 min (reproduced from ref 75).

(~50 nm) of mixed P*t*BA/PS brushes that were stained with RuO_4 vapor to enhance the contrast. For the high MW sample, the two grafted polymers in the brush layer (~20 nm) clearly underwent lateral microphase separation, forming a "rippled" nanostructure with the dark and white areas corresponding to PS and P*t*BA microdomains, respectively.[74] The feature size was ~10 nm, which is on the same order of $\langle R_{rms} \rangle$ of polymers in an ideal state (9.2 nm for P*t*BA having a M_n of 24.2 kDa and 10 nm for PS having a M_n of 23.0 kDa), consistent with the theoretical prediction, though the brushes were on curved substrates. The pattern formed was random and worm-like, resembling the early stage spinodal decomposition of polymer blends but at a much smaller scale. For the low MW sample, no clear phase separation can be seen in the brush layer from the TEM micrograph, consistent with the DSC result.

We further used TEM to study the phase morphologies of mixed P*t*BA/PS brush-grafted particles after exposure to different solvents.[75] Figure 3A shows a typical top-view TEM micrograph of the high MW sample, which was cast from chloroform, a good solvent for both P*t*BA and PS, and stained with RuO_4 vapor. As in the melt, this sample underwent lateral microphase separation, producing a nearly bicontinuous, random worm-like pattern. A distinct difference from the morphology in melt (Figure 2) is that both P*t*BA and PS were highly stretched and the interstitials among silica particles were completely covered by microphase-separated PS and P*t*BA chains. Moreover, the dark PS and white P*t*BA stripes bridged among neighboring particles. Figure 3B shows a typical TEM micrograph of the microtomed thin section (~50 nm). A "rippled" nanostructure can be clearly

seen. The thickness of the mixed brush layer was ~30 nm, which is in contrast to ~20 nm in the equilibrium melt state. We believe that the two grafted polymers phase-separated laterally in nonselective solvents, as suggested by theoretical studies.[28] However, to directly visualize the nanostructures of mixed brushes in a solvent, it is necessary to carry out cryogenic TEM studies. Completely different from the high MW sample shown in Figure 3, the low MW sample did not strongly microphase separate when cast from $CHCl_3$ (Figure 4), the same as in the melt state. Comparing the phase morphologies of two samples shown in Figures 2−4, it is clear that the critical MWs for the phase separation of mixed P*t*BA/PS brushes are between the molecular weights of two samples (ca. 10−23 kDa).

As mentioned earlier, various surface micellar structures have been predicted in theoretical and simulation studies but had not been directly visualized in the experimental studies. To induce the formation of surface-tethered micelles in the mixed P*t*BA/PS brushes, *n*-octane, which is a good solvent for P*t*BA but a poor solvent for PS, was slowly added into a dispersion of the high MW mixed P*t*BA/PS brush sample in $CHCl_3$ under strong stirring. After the removal of $CHCl_3$, PS chains collapsed, and its high T_g helped arrest the self-assembled nanostructure of mixed brushes in *n*-octane. Figure 5A−C shows typical TEM micrographs of the particles cast from *n*-octane. A striking difference from Figure 3A is that after the solvent evaporation the polymer chains were no longer highly stretched out and covered the interstitials among the particles. The nearly bicontinuous worm-like morphology observed in Figure 3 was transformed into a nanostructure composed of isolated (dark) PS microdomains in the (bright) P*t*BA matrix. Because *n*-octane is a poor solvent for PS, to minimize the contacts of PS segments from the unfavorable solvent, P*t*BA chains likely formed a shielding layer around the PS microdomains, yielding a surface-tethered micellar structure—the nanostructure predicted in the theoretical studies and illustrated in Scheme 1. Similar surface micelles were also observed in amphiphilic mixed PAA/PS brushes after water was gradually added into the dispersion of the hairy particles in DMF and the cast particles were stained with uranyl acetate (Figure 5D).

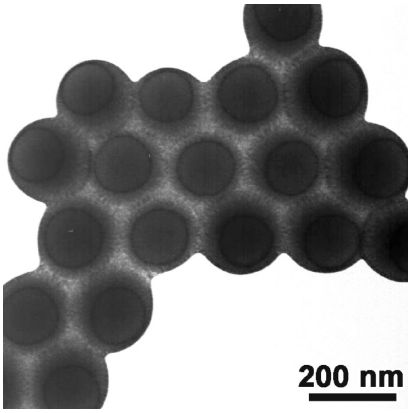

Figure 4. TEM micrograph of the low MW mixed P*t*BA/PS brush-grafted particles (P*t*BA M_n of 10.4 kDa and grafting density of 3.1 nm^2/P*t*BA chain; PS M_n of 11.9 Da and grafting density of 2.9 nm^2/PS chain) that were cast from $CHCl_3$, a good solvent for both P*t*BA and PS. The sample was stained with RuO_4 vapor for 30 min (reproduced from ref 75).

These studies showed that for the high MW mixed P*t*BA/PS brushes cast from $CHCl_3$ a random worm-like, nearly bicontinuous morphology was formed. In selective solvents (*n*-octane for mixed P*t*BA/PS and H_2O for mixed PAA/PS brushes), PS chains collapsed and packed into isolated domains shielded by the second polymer. These results confirmed the theoretical predictions of the formation of "rippled" nanostructures and surface micellar structures of mixed brushes induced by nonselective good solvents and selective solvents, respectively.

Although exciting progress has been made on the direct visualization of phase morphologies of mixed homopolymer brushes, there are still a lot of unanswered fundamental issues. Solving these issues will further enhance our understanding of how two polymers organize themselves in mixed brushes and enable a rational design of responsive materials by the use of mixed homopolymer brushes. These issues are listed below. (i) The substrate curvature effect on the microphase separation of mixed homopolymer brushes. In our work, we used silica particles with a diameter of 180 nm, and the $\langle R_{rms} \rangle$ of grafted polymers was ~10 nm. To ensure that the morphology of mixed brushes observed on such large particles is not affected by the particle size, it is necessary to use even larger particles as substrate to grow mixed brushes. One actually can use a mixture of silica particles with various sizes and carry out the reaction in one pot. (ii) The critical molecular weight for symmetric mixed homopolymer brushes to begin microphase separation. Marko and Witten predicted that the critical molecular weight for symmetric mixed brushes to phase separate is 2.27 times that for the same polymers in a simple blend.[27a] (iii) The correlation between the periodicity of the "rippled" nanostructure and the molecular weight of symmetric mixed brushes under constant grafting densities. According to the theoretical study,[27a] the ripple wavelength of the nanopattern is 1.97 times the $\langle R_{rms} \rangle$. A quantitative

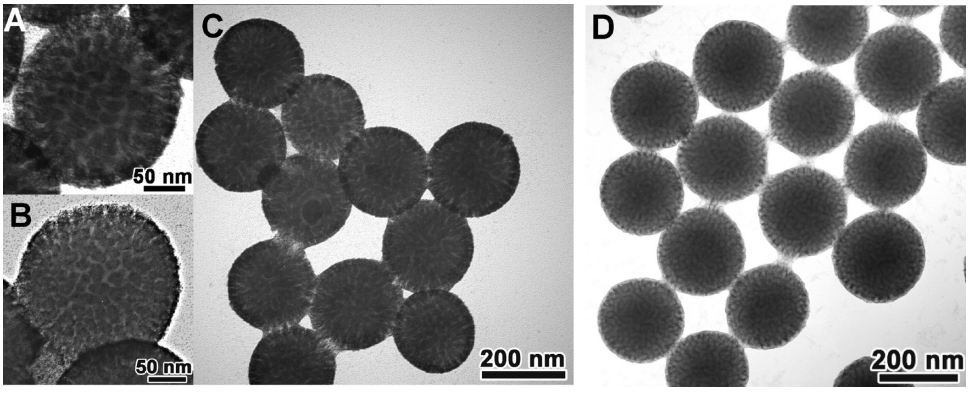

Figure 5. TEM micrographs of the high MW mixed P*t*BA/PS brush-grafted particles that were cast from *n*-octane, a selective solvent for P*t*BA (A−C), and mixed PAA/PS brush-grafted particles cast from water, a selective solvent for PAA (D). Micrographs (A) and (B) are magnified images showing the (dark) isolated PS microdomains in the (bright) continuous P*t*BA matrix. The mixed P*t*BA/PS brush samples were stained with RuO_4 vapor for 30 min. The mixed PAA/PS brush-grafted particles were stained with uranyl acetate. Mixed PAA/PS brush-grafted particles were synthesized from the high MW mixed P*t*BA/PS brush sample (P*t*BA M_n of 24.2 kDa and PS M_n of 23.0 kDa) by the removal of a *tert*-butyl group of P*t*BA (reproduced from ref 75).

Scheme 4. Microphase Separation of Symmetric Mixed Homopolymer Brushes at the (Curved) Substrate−Vacuum Interface: (a) Lateral, (b) Vertical, and (c) Vertical + "Hidden" Lateral

(a) Lateral (b) Vertical (c) Vertical + "Hidden" Lateral

analysis of Figure 3A showed that the average width of dark PS microdomains was 13.5 ± 4.7 nm, while that of bright P*t*BA microdomains was 8.2 ± 3.6 nm. The estimated values of $\langle R_{rms} \rangle$ of PS and P*t*BA having the same molecular weights as the grafted polymers in an ideal state are 10.0 and 9.2 nm, respectively. Thus, our results are almost in a quantitative agreement with theoretical predictions. Still, more work is needed to establish the scaling relationship between the chain length and the "ripple" wavelength. (iv) The effect of grafting density. It can be imagined that if the grafting density is low, the entropic loss associated with chains traveling in different regions of the laterally phase-separated brush layer may not be compensated by the energy decrease gained from the microphase separation. However, it is challenging to systematically change the overall grafting density while keeping the grafting densities of two polymers comparable. (v) The effect of relative chain lengths. It is possible that the morphology of mixed brushes in melt evolves from a layered structure to a bicontinuous rippled phase to a layered structure when the chain length of one polymer is held constant and the DP of another polymer is gradually increased. (vi) In Marko and Witten's work, it is implied that χ_{AE} is equal to χ_{BE} and χ_{AS} is equal to χ_{BS}. It can be imagined that interfacial free energy plays a role in the microphase separation of mixed homopolymer brushes, especially those composed of two polymers with very different surface free energies because it is known that the more hydrophobic component is enriched at the outermost layer in vacuum. Thus, there are three possibilities for the microphase separation as shown in Scheme 4. When the surface free energies of the two polymers are identical or very close, the two polymers undergo lateral microphase separation as predicted by Marko and Witten (Scheme 4a). If the surface free energy difference between two polymers is substantially large, the more hydrophobic species will be enriched at the topmost surface during thermal annealing in vacuum. Two scenarios can be envisioned: the two polymers phase separate vertically (Scheme 4b), where surface enriching is driven by different surface free energies of the two polymers; the two polymers phase separate laterally in the bottom layer, producing a hidden "rippled" nanostructure (Scheme 4c, vertical + lateral phase separation underneath the top layer). Similarly, if the affinity of one polymer to the substrate is stronger than another one, vertical phase separation is possible. However, the control and tuning of χ_{AS} and χ_{BS} is very challenging. (vii) As shown in Figures 2 and 3, the lateral microphase separation of mixed brushes in melt and a nonselective solvent produces a random worm-like, nearly bicontinuous nanopattern with no long-range order. The simulation studies indicated that the randomness of grafting sites prevents the formation of a long-range order.[28f,g] Even a small fluctuation is sufficient to disrupt the long-range order. It would be very interesting if mixed brushes can be induced to form ordered nanopatterns. In principle, this is possible if an external field (e.g., a lamella-forming block copolymer matrix or a nanopatterned wall with an appropriate feature size in contact with the brush) is applied to direct the microphase separation of mixed brushes.

Large mixed brush-grafted particles are of great interest to a number of technological applications including particle-stabilized emulsions of small molecule liquids or polymers and self-cleaning surfaces. Motornov et al. prepared amphiphilic

Scheme 5. A Solid Particle Is Residing at the Interface of A and B Phases with Contact Angle, Defined with Respect to Phase B, Smaller than, Equal to, and Larger than 90°

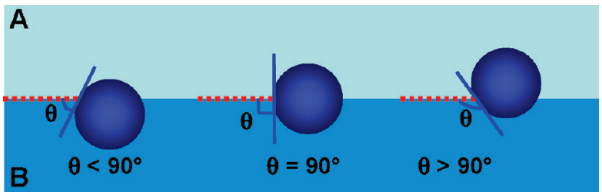

mixed brush-grafted particles by using a quaternization reaction between 200 nm silica particles or fused silica nanoparticle aggregates functionalized with 11-bromoundodecyltrimethoxysilane and the pyridine groups in a triblock copolymer PS-*b*-PVP-*b*-PEO.[10,76] Because of the random nature of the grafting reaction and only a small number of pyridine groups participating in the reaction, the obtained brushes were actually mixed block copolymer brushes constituted of grafted block copolymers PVP-*b*-PEO and PVP-*b*-PS.[10,76] Note that block copolymer brushes are another type of surface-responsive materials.[95] The responsive properties of these hairy particles manifested in the formation of stable dispersions in both toluene and water. In toluene, a good solvent for PS, PVP collapsed and PS blocks were stretched; PEO was presumably segregated between PS and PVP layers. In an aqueous solution with pH < 4, a good solvent for PVP and PEO and a poor solvent for PS, PS collapsed and PVP and PEO were stretched. In an aqueous solution with a pH > 4, PEO chains formed the corona, while PS and PVP collapsed. Interestingly, the interactions between hairy particles can be tuned by adjusting the solution pH; reversible aggregation−dispersion transitions in water were achieved by changing pH. Cheng et al. prepared mixed PS and poly(*tert*-butyl methacrylate) (P*t*BMA) brush-functionalized nanodiamond aggregates by grafting P*t*BMA-*b*-poly(glycidyl methacrylate)-*b*-PS with a short central block to the surface of nanodiamonds via the reaction between the epoxy groups in the central block and the carboxyl groups on the surface of nanodiamond aggregates.[78] The size of aggregates decreased from several micrometers to hundreds of nanometers after the surface immobilization reaction. Hydrolysis of P*t*BMA produced amphiphilic mixed PS/poly(methacrylic acid) (PMAA) brush-grafted particles.

It is known that solid nano- and microparticles can be used as surface active materials, though they do not necessarily have an amphiphilic feature as surfactants.[9b] The emulsions of water and oil formed with particles as stabilizers are traditionally called Pickering emulsions, which have found practical uses in cosmetics, controlled release, etc. As shown in Scheme 5, there are three possibilities for particles residing at an interface with the contact angle (θ) less than, equal to, or greater than 90°, depending on the affinity of the particles toward the B phase. The energy (ΔE) that is required to remove a particle from the interface is

$$\Delta E = \pi R^2 \gamma_{AB} (1 \pm \cos\theta)^2 \quad (1)$$

where R is the radius of the particle, γ_{AB} is the interfacial energy between phases A and B, and θ is the contact angle of the particle at the interface.[9b] The sign inside the parentheses is negative for removal of the particle into the B phase and positive for removal into the A phase. The type of emulsions is primarily determined by the wettability of particles at the interface; it is generally observed that a contact angle <90° favors the formation of an A-in-B emulsion and a contact angle >90° favors the formation of a B-in-A emulsion.

Amphiphilic mixed brush-grafted particles are excellent candidates as particulate stabilizers for Pickering emulsions; these particles may exhibit synergistic stabilization abilities of

both *amphiphilic surfactant* and *solid particles*. Motornov et al. used their hairy particles as stabilizers for water−toluene Pickering emulsions.[10] It was found from conductivity measurements that o/w emulsions of toluene and water were formed at pH ≤ 3, while w/o emulsions were formed at pH ≥ 4. The particles were more hydrophilic at an acidic pH because of the protonation of PVP, favoring the formation of an oil-in-water emulsion. At pH higher than 4, the hairy particles became less hydrophilic, causing the formation of a water-in-oil emulsion. Thus, the type of emulsions can be changed by adjusting the pH of the water phase, an excellent example demonstrating the potential of amphiphilic mixed brush-grafted particles as environmentally responsive Pickering emulsion stabilizers. Cheng et al. also showed that mixed PS/PMAA brush-grafted nanodiamond aggregates can act as an environmentally responsive stabilizer for Pickering emulsions of water and chloroform.[78] At pH > 10, the particles were found only in the water phase. When the pH was decreased to < 5, the particles resided at the interface, forming o/w droplets.

Superhydrophobic and superhydrophilic surfaces have attracted increasing attention in recent years because of their self-cleaning abilities. These surfaces are usually made by using surface roughness to amplify the surface wettability, making a hydrophobic surface more "hydrophobic" and a hydrophilic surface more "hydrophilic".[46] Hairy particles are natural candidates for the fabrication of self-cleaning materials as coating a substrate with hairy particles modifies its surface chemical composition and simultaneously introduces surface roughness if particles with a right size are used. Moreover, for amphiphilic mixed brush-grafted particles, the surface wettability can be switched between hydrophilic and hydrophobic by exposing the surface to different solvents or by heating. Motornov et al. showed that superhydrophobic coatings can be made by depositing their mixed brush-grafted silica particles onto a polyamide textile sample.[10] Upon heating above the T_g of PS, the surface exhibited an advancing contact angle of 154° and a roll-off angle of less than 11°. The surface can be switched to a hydrophilic state by exposure to an acidic aqueous solution. However, the deposition of the same particles onto silicon wafers did not produce a superhydrophobic coating, indicating that the substrate texture played an important role. Motornov et al. also prepared mixed polymer brush-grafted particles by grafting PS-*b*-poly(4-vinylpyridine) to ∼150 nm particles composed of 14 nm fused silica nanoparticles and functionalized with bromoalkyl groups.[77] They observed that increasing the pH above 5 caused the formation of hierarchically structured aggregates of hairy particles. Deposition of the aggregates onto flat substrates and subsequent heating produced superhydrophobic coatings. Note that these superhydrophobic surfaces were made from environmentally benign water-borne dispersions. The coatings can be easily switched to a hydrophilic state upon exposure to acidic water (pH = 3) and back to the superhydrophobic state by heating in air or by exposure to toluene. In principle, one should be able to make superhydrophobic/superhydrophilic coatings by directly depositing amphiphilic mixed brush-grafted particles onto a substrate without resorting to the substrate texture or the secondary aggregates of hairy particles. More work is needed to optimize the conditions. Also, to make the coating permanent, a polymer that can form covalent bonds with substrates may be used in the preparation of mixed brush-grafted particles.

Mixed Brush-Grafted Particles with a Core Radius Smaller than the $\langle R_{rms} \rangle$s of Grafted Polymers

Mixed brush-grafted particles with a core radius smaller than the $\langle R_{rms} \rangle$s of grafted polymers not only exhibit responsive properties as large particles discussed in the previous section but also possess some unique characteristics. They could act as Janus particles, the particles having two physically or chemically differing sides/surfaces, more effectively via phase separation at an interface as the grafted chains are long enough to extend to the other side of the particle (Scheme 6). Note that in principle large mixed brush-grafted particles can also behave as Janus particles at an interface via the formation of micelles and inverted micelles on the opposite sides of particles (Scheme 6). This unique feature of small particles enables them to self-assemble into novel hierarchical structures that are not accessible to large mixed brush-grafted particles. We will repeatedly come back to this point in the following discussions of mixed brush-grafted particles at the water−air interface, in a solvent selective for one polymer, and at the polymer−polymer interface.

Scheme 6. Mixed Homopolymer Brush-Grafted Particles Behaving as Janus Particles at an Interface of A and B Phases

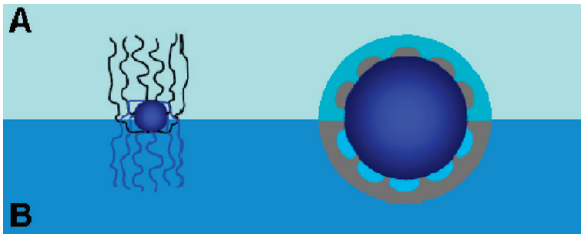

There have been a number of reports on mixed polymer brushes on metal and inorganic nanoparticles with a size of several nanometers.[79−87] Most of these hairy hybrid nanoparticles were prepared by "grafting to" methods, either directly using two distinct end-functionalized polymers as stabilizing ligands in the synthesis of nanoparticles or grafting functionalized polymers to the surface of particles.[79−84] Other methods, for example, direct synthesis of quantum dots in the core of the micelles of an ABC triblock copolymer with the short B block forming the core and the other two blocks forming the corona,[85,86] have also been used for the synthesis of mixed brush-grafted particles.

Shan et al. reported a "grafting to" method to prepare amphiphilic PS- and poly(*N*-isopropylacrylamide) (PNIPAm)-grafted gold nanoparticles.[79−81] They found that the RAFT polymers bearing a dithioester end group can be used directly as ligands for the synthesis of gold nanoparticles because the dithioester end group can be reduced to a thiol under the reduction conditions for $HAuCl_4$. The gold nanoparticles synthesized by this method were 2−3 nm in diameter, determined by TEM.[79] The molar ratio of two polymers on the particles can be tuned by changing the feed ratio. The monolayer behavior of amphiphilic hairy nanoparticles at the air−water interface was studied using a Langmuir film balance. The compression isotherm of hairy particles with comparable molar contents of PS and PNIPAm showed several characteristic regions that can be attributed to the polymer conformational transitions from the pancake, the pancake to brush transition, to the brush. Note that PS-grafted nanoparticles cannot form a stable monolayer at the water−air interface. Presumably, PNIPAm chains were immersed in the water subphase and PS chains were in air, producing a Janus nanostructure (Scheme 7).[80] The optical properties of Langmuir monolayer were studied by in-situ spectroscopy analysis. Upon compression in the Langmuir trough, the surface plasmon resonance (SPR) bands for mixed brush-grafted Au nanoparticles at 20 and 30 °C exhibited a blue shift. It was concluded that the blue shift was induced by compression and closely related to the conformational change of the PNIPAm chains.

Using a mixture of two end-functionalized polymers as ligands to prepare binary mixed brush-grafted nanoparticles is a simple and straightforward process; the ratio and molecular weights of

Scheme 7. Amphiphilic Mixed PS/PNIPAm Brush-Grafted Gold Nanoparticles at the Water−Air Interface upon Compression[a]

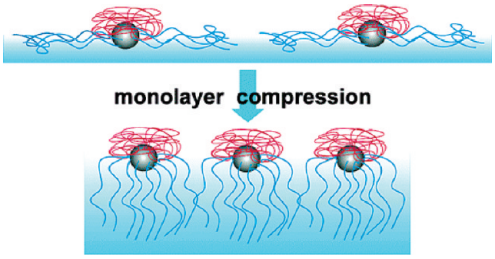

[a] The hairy particles underwent microphase separation, producing amphiphilic Janus particles (reproduced from ref 80).

two ligands can be tuned. However, it is unclear how the grafting sites of two polymers are distributed on the surface of nanoparticles. Zubarev et al. reported a "grafting to" method that produces truly mixed homopolymer brush-grafted nanoparticles,[82−84] in which two polymers are alternately immobilized by one end on the surface. Their method involved grafting a diblock copolymer with a carboxylic acid group at the junction point of the two blocks to 4-mercaptophenol-stabilized gold nanoparticles via a DCC-type coupling reaction, producing V-shaped amphiphilic mixed polybutadiene (PB)/poly(ethylene oxide) (PEO) or PS/PEO brushes.[82,83] On the basis of the weight gain after grafting, the molecular weight of diblock copolymer, and the assumption that 2 nm gold nanoparticles contained 270 atoms, the grafting density of mixed PB/PEO brushes was found to be 2.94 chains/nm^2.[82] The responsive properties of mixed PB/PEO brush-grafted nanoparticles can be seen from their ability to be dispersed in a broad range of solvents, including such extremes as pure hexane and pure water. The dispersions were very stable over a long period of time.

The self-assembly of amphiphilic mixed homopolymer brush-grafted gold nanoparticles in solution is particularly interesting. For example, after water was added dropwise to a THF solution of V-shaped PS/PEO brush-grafted Au nanoparticles with PS M_n = 4000 Da and PEO M_n = 2200 Da (the final solution contained 75 vol % of water) and the mixture was dialyzed against water to remove THF, well-defined rod-like nanoassemblies with a diameter of 18 nm and ∼100 nm in length were observed by TEM (Figure 6).[83] The particles were residing with an average interparticle distance of ∼3 nm at the interface, i.e., the boundary separating the insoluble glassy PS core from the solubilizing PEO chains. The radius of nanorods was in good agreement with the length of PS chains in the fully extended, all-trans conformation, suggesting that the diameter of nanorod assemblies was determined by the PS chain length. This was supported by the observation that the nanorod diameter was bigger when longer hydrophobic PS was used. Interestingly, when larger gold nanoparticles were used, the hairy particles form irregular aggregates in water. It appears that to form rod-like nanoassemblies the lengths of polymer chains need to be sufficiently greater than half circumference of the particles so that the hairy particles can rearrange into Janus hairy particles via microphase separation. Although hairy particles with a large core can also act as Janus particles via the formation of micelles and inverted micelles on the opposite sides of the core (Scheme 6), particles with a small core and a long hair appear to behave more effectively as Janus particles. The interfacial behavior of amphiphilic PB/PEO brush-grafted gold nanoparticles was examined by using Langmuir−Blodgett techniques.[84] These nanoparticles can form stable Langmuir monolayers at the air−water interface through phase segregation with hydrophobic PB chains pointing toward air and hydrophilic PEO chains being

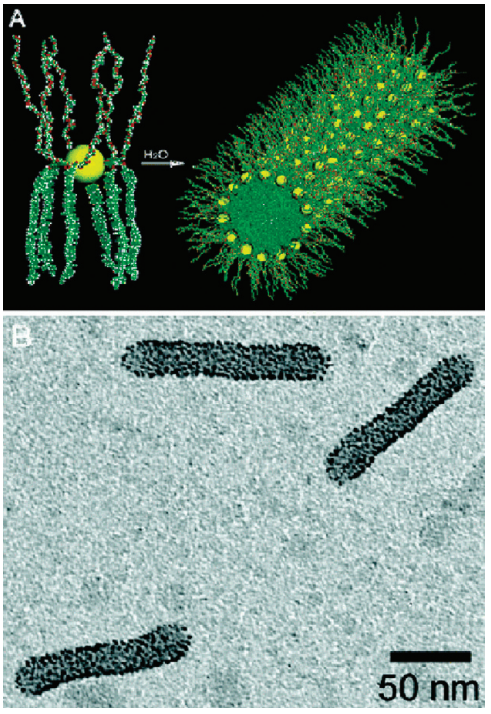

Figure 6. (A) Schematic representation of the self-assembly of mixed PS/PEO brush-grafted Au nanoparticles in water. (B) TEM image of a sample prepared from an aqueous solution of mixed PS/PEO brush-grafted nanoparticles after dialysis of a THF/H_2O (1:3 v/v) solution against DI water (reproduced from ref 83).

immersed in water, similar to the mixed PS/PNIPAm brush-grafted Au nanoparticles at the water−air interface investigated by Shan et al.[80]

Using a different approach, Guo and Moffitt synthesized semiconductor quantum dots (QDs) functionalized with binary mixed PS/PMMA brushes.[85,86] Their synthesis started from the micellization of a triblock copolymer PS_{296}-*b*-PAA_{41}-*b*-$PMMA_{236}$ in a mixture of benzene/methanol (9:1 v/v) induced by addition of cadmium acetate, which neutralized the PAA block, resulting in the formation of insoluble poly(cadmium acrylate) ionic cores surrounded by a mixed corona of PS and PMMA chains. Subsequent reaction with H_2S produced CdS QDs with a mixed PS/PMMA brush layer. From TEM analysis, the diameter distribution of QDs was bimodal with a larger particle population centered at 7 nm and a smaller population at ∼4 nm, which might be because, in a majority of micelles, all Cd^{2+} ions were converted to a single QD, whereas some micelles contained multiple smaller QDs due to the incomplete reaction.

The obtained hybrid particles can be easily dispersed in organic solvents of various polarities including acetone, chloroform, THF, and toluene, yielding clear colloidal dispersions. Note that pure PS-grafted quantum dots cannot form a stable dispersion in acetone, which is a selective solvent for PMMA. The environmentally responsive properties of the particles also manifested in their capability of being dispersed in both PS and PMMA homopolymers. UV−vis spectroscopy and photoluminescence studies showed that QD sizes and optical properties were independent of solvent media because of the protection provided by the mixed brush layer. 2D ^{1}H nuclear Overhauser effect spectroscopy (NOESY) analysis, which can probe through-space dipolar interactions of proximal protons (<0.5 nm), was employed to investigate whether PS and PMMA chains were mixed or compartmentalized within the brush layer. The results showed that PS and PMMA were randomly distributed within the brush layer in THF-d_8. However, ^{1}H NOESY spectroscopy analysis

cannot tell whether mixed PS/PMMA brushes phase-separated or not because even in the microphase-separated state of alternately grafted binary mixed brushes, there is a crossover zone in which PS and PMMA segments are in an intimate contact, which would produce signals in 2D ^{1}H NOESY spectra. Controlling the phase morphology of polymer blends is very important for many technological applications. Guo and Moffitt applied their hairy CdS QDs as a stabilizer for PS/PMMA binary polymer blends by taking advantage of the responsive properties of mixed brush-grafted particles.[86] The hairy particles can self-assemble at the polymer/polymer interface in phase-separating PS/PMMA blends. The segregated QDs regulated the phase separation during spin-coating and dramatically stabilized the spin-coated blend morphologies in the subsequent annealing. This is in a sharp contrast with neat PS/PMMA blends which underwent rapid phase inversion and coarsening. Moreover, the QDs retained their photoluminescence after the interfacial self-assembly and subsequent annealing.

The two distinct polymers in a mixed brush can be stimuli-responsive polymers, e.g., thermosensitive water-soluble polymers; these mixed brushes and hairy particles could exhibit interesting properties that are different from conventional mixed homopolymer brushes. Very recently, Boyer et al. reported the preparation of doubly thermosensitive mixed brush-grafted gold nanoparticles.[87] The thermosensitive polymers used in this work were (co)polyacrylates with a short oligo(ethylene glycol) pendant from each repeat unit, which belong to a new class of thermosensitive water-soluble polymers.[96] Two different thermosensitive polymers, poly(ethoxydi(ethylene glycol) acrylate) (PDEGA) with a LCST of ~15 °C and poly(DEGEA-*co*-oligo(ethylene glycol) acrylate) (P(DEGA-*co*-OEGA)) with a LCST of ~33 °C which were synthesized by RAFT, were assembled onto gold nanoparticles directly via ligand exchange due to the strong affinity of the trithiocarbonate chain end of RAFT polymers to the gold surface. The thermoresponsive properties of the particles were investigated. As the temperature increased slowly from 5 to 25 °C, no significant change was observed in the plasmon absorbance from UV−vis spectrometry and there was only a very slight decrease in the size of hairy particles. When the temperature reached 28−30 °C, slightly lower than the second LCST (~33 °C), the size increased quickly from 35 to 250 nm, and the solution color changed from red to purple, indicating that the particles underwent aggregation. Fluorescence spectroscopy was employed to further study the LCST transitions of hairy particles using pyrene as probe. It is known that when pyrene is sequestered in a hydrophobic environment, there is a decrease in the intensity ratio of the first I_1 to the third I_3 vibration bands. For mixed PDEGA/P(DEGA-*co*-OEGA) brush-grafted gold nanoparticles, the ratio I_1/I_3 versus temperature is shown in Figure 7. Two transitions were observed: the first one occurred at 8−10 °C and the second one at 25−28 °C, which corresponded to the LCST transitions of two grafted polymers in the brush layer. The transitions were reversible. Although two LCSTs transitions have been detected, it is unclear how the two polymers self-assemble in the mixed brush layer when one or both polymers collapse.

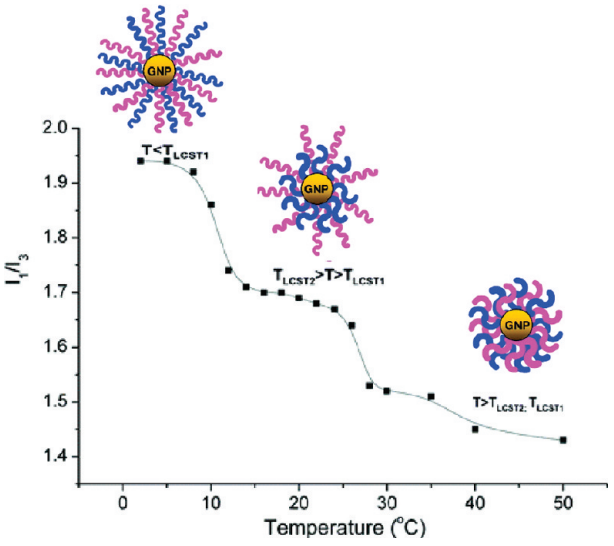

Figure 7. Evolution of the I_1/I_3 ratio of pyrene versus temperature for gold nanoparticles grafted with mixed polymer brushes composed of PDEGA with a LCST of 15 °C and P(DEGA-*co*-OEGA) with a LCST of ~33 °C (reproduced and adapted from ref 87).

Mixed Brush-Grafted Particles with a Core Radius Comparable to the $\langle R_{rms} \rangle$ of Grafted Polymers

The curvature of core particles is expected to affect the phase behavior of two grafted polymers in the brush layer. Unlike on planar substrates, the segments of the polymers grafted on a curved substrate are densely packed near the grafting sites but have more space with increasing the distance from the particle surface. However, the substrate curvature effect on the phase separation of mixed brushes has not been systematically studied.

Using computer simulation, Roan investigated the microphase separation of immiscible mixed homopolymer brushes on spherical nanoparticles with a radius comparable to the polymer size $\langle R_{rms} \rangle$, and very rich morphologies were revealed.[73] By varying polymer chain lengths, grafting densities, and grafting patterns, well-ordered 3-, 6-, 8-, 9-, 10-, and 12-island structures can form in the microphase-separated spherical mixed brushes, resulting in soft nanopolyhedras with structures similar to those found in small clusters of colloidal microspheres.[97] For example, the equilibrium nanostructures can be changed from rippled, to 12-islanded, and then layered with the increase of chain length disparity under the condition that the grafting densities for A and B are identical (Figure 8). On the other hand, when the grafting densities for the two polymers are very different, a layered structure was observed with the minority chains extending farther away from the nanoparticle surface. On the basis of these results, Roan suggested a route to fabricate multivalent nanoparticles, namely, nanoparticles with precisely controlled numbers and locations of functional sites. These types of patterned soft particles are very interesting and could have potential applications in many fields such as the fabrication of drug carriers. However, this regime, in which the core size is in the range of tens of nanometers, remains as an "experimentally uncharted, intermediate territory",[73] partly because of the difficulty in the synthesis of well-defined high-density mixed homopolymer brushes on such sized nanoparticles. Moreover, the ordered nanostructures were predicted for the system in a nonselective good solvent for both polymers. Characterization of such structures will be challenging, though cryo-TEM might be very useful. Despite the synthesis and characterization challenges, if multivalent nanoparticles are formed and detected, a broad range of new possibilities will be opened up as these nanoparticles are similar to the patchy nanoparticles that have been theoretically discussed.[98] In addition, multivalent particles can be permanently fixed by cross-linking of both polymers and the core can be removed, leading to nanocages with the wall composed of two types of nanodomains. Note that ordered nanopatterns were observed by Stellacci et al. in self-assembled monolayers of thiols on gold nanoparticles.[99]

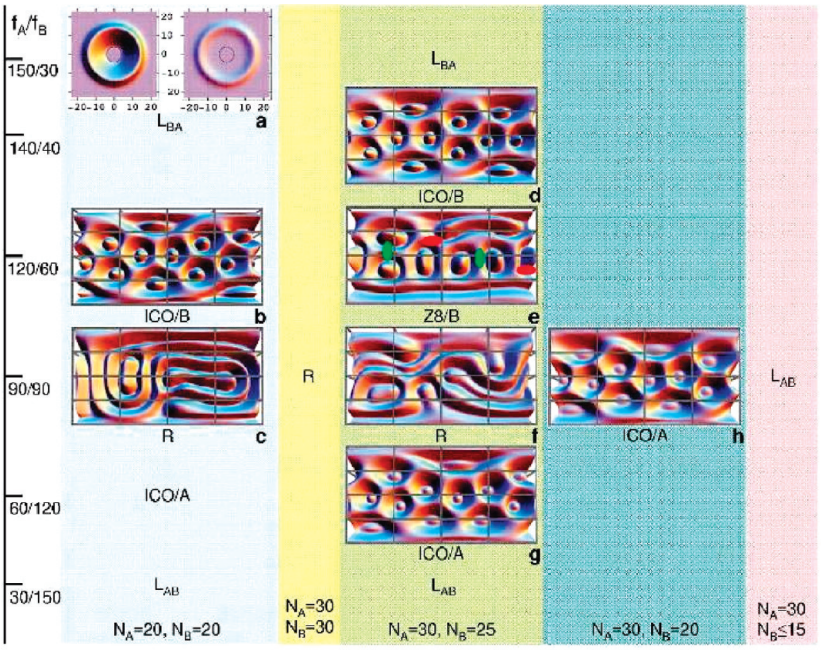

Figure 8. Structures at varying compositions but fixed total grafting density, $f_A + f_B = 180$, where f_A and f_B are the numbers of chains A and B, respectively. N_A and N_B are grafted chain lengths. (a) Free-end distributions of A (left) and B (right). (b)−(h) World maps of total segment density, $r = 7$. The radius of particles is 4, and Flory−Huggins interaction parameters between A and B, A and solvent, and B and solvent are 1, 0, and 0, respectively. Reprinted with permission from ref 73. Copyright 2006 the American Physical Society.

A special case of mixed brush-grafted particles with a core radius comparable to the polymer size is that both core and polymer are very small, only a few nanometers. Chiu et al. prepared binary PS and PVP-grafted gold nanoparticles by standard reduction of $HAuCl_4$ in THF or two phase toluene/water using low molecular weight thiol-terminated PS ($M_n \sim 1300$ Da, PDI = 1.10) and PVP ($M_n \sim 1500$ Da, PDI = 1.09) chains as stabilizing ligands.[88] The average core diameter of gold nanoparticles was 3.9 ± 1.0 nm, and the polymer shell thickness was ~1.9 nm. Compared with either pure PS- or pure PVP-coated nanoparticles, binary brush-grafted particles exhibited different behavior when dispersed in a PS-*b*-PVP lamellar diblock copolymer phase. Pure PS- and PVP-coated gold nanoparticles were found to be localized in the center of the PS and PVP nanodomains of PS-*b*-PVP, respectively.[88] This is understandable because by segregating into the corresponding domain of the block copolymer, the particles lower their enthalpy, and by concentrating particles near the center of the compatible domain where the polymer chain ends are located, the chains can accommodate particles by moving apart rather than by stretching. In contrast, the particles that were grafted with a mixture of PS and PVP thiols were localized at the interface between PS and PVP nanodomains. This interfacial adsorption can be explained by using eq 1 if we consider that the difference between the interfacial free energies of PS and the nanoparticle and of PVP and the nanoparticle is very small (i.e., $\cos\theta \ll 1$). The estimated adsorption energy of a nanoparticle at the PS−PVP interface is $E_a = 10\ k_BT$,[88] which drives the nanoparticles to the interface.

Theoretically, any nanoparticles with an approximately "neutral" surface relative to PS and PVP will adsorb to the interface. This was supported by the observation that Au nanoparticles coated with a thiol-terminated random copolymer P(S-*r*-VP) with a PS molar fraction of 0.52 were localized at the interfaces in PS-*b*-PVP.[89] A difference between the particles grafted with a mixture of PS and PVP and the particles grafted with a P(S-*r*-VP) is that the binary PS and PVP brushes could phase separate, and

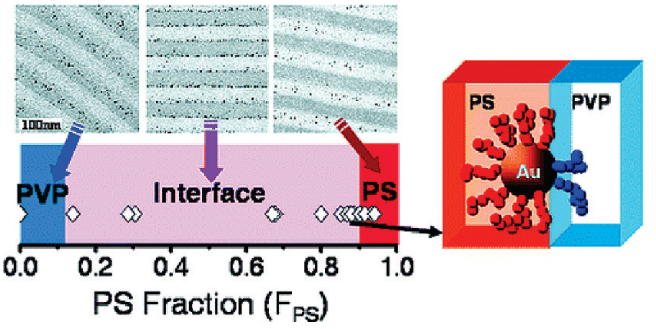

Figure 9. Segregation of binary PS- and PVP-coated Au nanoparticles with varying surface compositions (F_{PS}: mole fraction of PS) in a microphase-separated diblock copolymer PS-*b*-PVP (reproduced from ref 90).

the hairy particles may behave as Janus particles at the interface. However, with such short polymer chains, it is unlikely that PS and PVP will undergo a microphase separation as illustrated in Scheme 6. Kim et al. synthesized a library of binary low-molecular-weight PS and PVP brush-grafted Au nanoparticles with varying PS and PVP surface compositions (F_{PS}) and incorporated them into a lamellar PS-*b*-PVP diblock copolymer.[90] Sharp transitions in the particle location from the PS domain to the PS/PVP interface, and subsequently to the PVP domain, were observed at $F_{PS} = 0.9$ and 0.1, respectively. This extremely wide window of F_{PS} values at which binary PS and PVP brush-coated Au nanoparticles adsorbed to the interface suggests a redistribution of PS and PVP on the Au surface (via surface diffusion), producing Janus nanoparticles at the PS/PVP interfaces (Figure 9). A calculation for the adsorption energy to the interface of nanoparticles with different surface arrangements of PS and PVP ligands supports the rearrangement of thiol-terminated homopolymers. An upper limit estimation of the adsorption energy of nanoparticles uniformly coated with a random arrangement of PS and PVP ligands where a 10% surface area was occupied by PVP was ~1 k_BT,[90] indicating that such

nanoparticles are unlikely to be segregated at the interface, in contrast to the experimental results for nanoparticles coated with binary PS and PVP brushes.

Concluding Remarks and Outlook

Mixed brush-grafted particles are an intriguing class of environmentally responsive hybrid nanostructured materials; these hairy particles are of great interest to both fundamental research and technological applications. In terms of morphology of mixed homopolymer brushes, although some exciting progress has been made in recent years, many fundamental issues remain unsolved or unexplored. In particular, no systematic theoretical and experimental studies have been performed on the substrate curvature effect on phase morphology of mixed homopolymer brushes under the equilibrium melt conditions and in solvents. Note that to describe a curved surface, it is necessary to use two radii of curvature, which are perpendicular to each other; they are equal for a sphere but not necessarily for other shaped objects. Besides spherical particles, the phase behavior of mixed homopolymer brushes on other shaped nano-objects, e.g., nanorods which have one finite radius of curvature and one infinite radius of curvature, is also of great interest. However, no theoretical or experimental studies have been performed on mixed homopolymer brushes on nanorods. Intuitively, if the nanorod diameter is comparable to the polymer size, there is a possibility that mixed brushes phase separate into alternating rings. It would be of great interest if one ring is hydrophobic and another one is hydrophilic, an interesting hairy hybrid nano-object that could find technological applications (e.g., site-isolated catalysts[100,101]). In addition, the morphology of mixed homopolymer brushes on a concave surface, e.g., on the surface of nanopores of tens of nanometers, is unknown. If the radius of curvature is comparable to the $\langle R_{rms} \rangle$s of polymers, the interactions of grafted polymers with both substrate surface and grafted polymers on the opposite side of the nanopore may become important in the determination of self-assembled nanostructures of symmetric mixed brushes in melt and in solvents. Thus, various interesting phase morphologies could be observed when the substrate of mixed homopolymer brushes is changed from a flat solid substrate, to a spherical particle with a radius significantly larger than, comparable to, and smaller than the polymer size, to a nanorod, and a concave substrate.

Moreover, mixed brushes could be extended from mixed homopolymer brushes to mixed block copolymer brushes. For example, Dong et al. have investigated the phase behavior of mixed block copolymer brushes that contain equal numbers of A−B diblock copolymer chains and complementary B−A chains that are densely grafted to a surface in the melt state using mean-field methods.[102] The demixing leads to a density wave of composition, produced by splaying of the polymer chains. The synthesis of such mixed block copolymer brushes is technically feasible, e.g., by using sequential surface-initiated ATRP and NMRP from a Y-initiator-functionalized surface. ATRP and NMRP are "living"/controlled radical polymerization techniques, allowing the synthesis of diblock copolymers.

The potential of mixed polymer brushes and mixed brush-grafted particles has certainly not been fully tapped, though they have been used in the fabrication of switchable (super)hydrophobic/(super)hydrophilic smart surfaces, Pickering emulsions, environmentally responsive lithography, transport of particles across liquid−liquid interface, etc. Considering various parameters including chain lengths, overall and relative grafting density, surface chemical compositions, surface free energy of each polymer, substrate curvature, etc., mixed homopolymer brushes are simply a polymer system with high design flexibility. Using stimuli-responsive polymers to make mixed brushes would further enhance the phase behavior and responsive properties of mixed polymer brushes.

Experimental studies on mixed brushes began only 10 years ago and investigations on mixed brush-grafted particles only a few years ago. We have every reason to believe that in the near future we will have a better understanding of phase behavior of mixed brushes on solid substrates with various curvatures and the hierarchical self-assembly of mixed brush-grafted particles and will see more innovative applications of mixed polymer brushes.

Acknowledgment. B.Z. thanks the University of Tennessee, Knoxville (UTK), Petroleum Research Fund (PRF# 40084-G7), Ralph E. Powe Junior Faculty Enhancement Award, and NSF (DMR-0605663 and DMR-0906913) for supporting his research since he started his independent career at UTK. B.Z. is indebted to his co-workers at UTK.

References and Notes

(1) (a) Halperin, A.; Tirrell, M.; Lodge, T. P. *Adv. Polym. Sci.* **1992**, *100*, 31–71. (b) Zhao, B.; Brittain, W. J. *Prog. Polym. Sci.* **2000**, *25*, 677–710. (c) Tsujii, Y.; Ohno, K.; Yamamoto, S.; Goto, A.; Fukuda, T. *Adv. Polym. Sci.* **2006**, *197*, 1–45.

(2) (a) Prucker, O.; Rühe, J. *Macromolecules* **1998**, *31*, 592–601. (b) Prucker, O.; Rühe, J. *Macromolecules* **1998**, *31*, 602–613. (c) von Werne, T.; Patten, T. E. *J. Am. Chem. Soc.* **1999**, *121*, 7409–7410. (d) Pyun, J.; Matyjaszewski, K. *Chem. Mater.* **2001**, *13*, 3436–3448. (e) Jiang, X. M.; Wang, B. B.; Li, C. Y.; Zhao, B. *J. Polym. Sci., Part A: Polym. Chem.* **2009**, *47*, 2853–2870.

(3) (a) Ohno, K.; Koh, K.; Tsujii, Y.; Fukuda, T. *Angew. Chem., Int. Ed.* **2003**, *42*, 2751–2754. (b) Wang, B. B.; Li, B.; Zhao, B.; Li, C. Y. *J. Am. Chem. Soc.* **2008**, *130*, 11594–11595.

(4) (a) Guerrini, M. M.; Charleux, B.; Vairon, J.-P. *Macromol. Rapid Commun.* **2000**, *21*, 669–674. (b) Jayachandran, K. N.; Takacs-Cox, A.; Brooks, D. E. *Macromolecules* **2002**, *35*, 4247–4257. (c) Zhao, B.; Jiang, X. M.; Li, D. J.; Jiang, X. G.; O'Lenick, T. G.; Li, B.; Li, C. Y. *J. Polym. Sci., Part A: Polym. Chem.* **2008**, *46*, 3438–3446.

(5) Mulvihill, M. J.; Rupert, B. L.; He, R. R.; Hochbaum, A.; Arnold, J.; Yang, P. D. *J. Am. Chem. Soc.* **2005**, *127*, 16040–16041.

(6) (a) Farmer, S. C.; Patten, T. E. *Chem. Mater.* **2001**, *13*, 3920–3926. (b) Sill, K.; Emrick, T. *Chem. Mater.* **2004**, *16*, 1240–1243.

(7) (a) Vestal, C. R.; Zhang, Z. J. *J. Am. Chem. Soc.* **2002**, *124*, 14312–14313. (b) Matsuno, R.; Yamamoto, K.; Otsuka, H.; Takahara, A. *Macromolecules* **2004**, *37*, 2203–2209.

(8) Russell, T. P. *Science* **2002**, *297*, 964–967.

(9) (a) Binks, B. P.; Murakami, R.; Armes, S. P.; Fujii, S. *Angew. Chem., Int. Ed.* **2005**, *44*, 4795–4798. (b) Binks, B. P. *Curr. Opin. Colloid Interface Sci.* **2002**, *7*, 21–41.

(10) Motornov, M.; Sheparovych, R.; Lupitskyy, R.; MacWilliams, E.; Hoy, O.; Luzinov, I.; Minko, S. *Adv. Funct. Mater.* **2007**, *17*, 2307–2314.

(11) Wu, T.; Zou, G.; Hu, J.; Liu, S. *Chem. Mater.* **2009**, *21*, 3788–3798.

(12) (a) Chanana, M.; Jahn, S.; Georgieva, R.; Lutz, J.-F.; Baümler, H.; Wang, D. *Chem. Mater.* **2009**, *29*, 1906–1914. (b) Papaphilippou, P.; Loizou, L.; Popa, N. C.; Han, A.; Vekas, L.; Odysseos, A.; Krasia-Christoforou, T. *Biomacromolecules* **2009**, *10*, 2662−2671.

(13) Zhu, M.-Q.; Wang, L.-Q.; Exarhos, G. J.; Li, A. D. Q. *J. Am. Chem. Soc.* **2004**, *126*, 2656–2657.

(14) (a) Ejaz, M.; Yamamoto, S.; Ohno, K.; Tsujii, Y.; Fukuda, T. *Macromolecules* **1998**, *31*, 5934–5936. (b) Husseman, M.; Malmstrom, E. E.; McNamara, M.; Mate, M.; Mecerreyes, D.; Benoit, D. G.; Hedrick, J. L.; Mansky, P.; Huang, E.; Russell, T. P.; Hawker, C. J. *Macromolecules* **1999**, *32*, 1424–1431. (c) Matyjaszewski, K.; Miller, P. J.; Shukla, N.; Immaraporn, B.; Gelman, A.; Luokala, B. B.; Siclovan, T. M.; Kickelbick, G.; Vallant, T.; Hoffmann, H.; Pakula, T. *Macromolecules* **1999**, *32*, 8716–8724. (d) Kim, J.-B.; Bruening, M. L.; Baker, G. L. *J. Am. Chem. Soc.* **2000**, *122*, 7616–7617. (e) Wu, T.; Efimenko, K.; Genzer, J. *J. Am. Chem. Soc.* **2002**, *124*, 9394–9395. (f) Yu, W. H.; Kang, E. T.; Neoh, K. G. *Langmuir* **2004**, *20*, 8294–8300. (g) Advincula, R.; Zhou, Q.; Park, M.; Wang, S.; Mays, J.; Sakellariou, G.; Pispas, S.; Hadjichristidis, N. *Langmuir* **2002**, *18*, 8672–8684. (h) Jones, D. M.; Brown, A. A.; Huck, W. T. S. *Langmuir* **2002**, *18*, 1265–1269. (i) Ma, H. W.; Li, D. J.; Sheng, X.; Zhao, B.; Chilkoti, A. *Langmuir* **2006**, *22*, 3751–3756.

(15) Matyjaszewski, K.; Xia, J. H. *Chem. Rev.* **2001**, *101*, 2921–2990.

(16) Hawker, C. J.; Bosman, A. W.; Harth, E. *Chem. Rev.* **2001**, *101*, 3661–3688.

(17) (a) Moad, G.; Rizzardo, E.; Thang, S. H. *Aust. J. Chem.* **2005**, *58*, 379–410. (b) Moad, G.; Rizzardo, E.; Thang, S. H. *Acc. Chem. Res.* **2008**, *41*, 1133–1142.

(18) (a) von Werne, T.; Patten, T. E. *J. Am. Chem. Soc.* **2001**, *123*, 7497–7505. (b) Pyun, J.; Matyjaszewski, K.; Kowalewski, T.; Savin, D.; Patterson, G.; Kickelbick, G.; Huesing, N. *J. Am. Chem. Soc.* **2001**, *123*, 9445–9446. (c) Perruchot, C.; Khan, M. A.; Kamitsi, A.; Armes, S. P. *Langmuir* **2001**, *17*, 4479–4481. (d) Pyun, J.; Jia, S.; Kowalewski, T.; Patterson, G. D.; Matyjaszewski, K. *Macromolecules* **2003**, *36*, 5094–5104. (e) Blomberg, S.; Ostberg, S.; Harth, E.; Bosman, A. W.; van Horn, B.; Hawker, C. J. *J. Polym. Sci., Part A: Polym. Chem.* **2002**, *40*, 1309–1320. (f) Bartholome, C.; Beyou, E.; Bourgeat-Lami, E.; Chaumont, P.; Zydowicz, N. *Macromolecules* **2003**, *36*, 7946–7952. (g) Parvole, J.; Laruelle, G.; Guimon, C.; Francois, J.; Billon, L. *Macromol. Rapid Commun.* **2003**, *24*, 1074–1078. (h) Ohno, K.; Morinaga, T.; Takeno, S.; Tsujii, Y.; Fukuda, T. *Macromolecules* **2006**, *39*, 1245–1249. (i) Morinaga, T.; Ohno, K.; Tsujii, Y.; Fukuda, T. *Macromolecules* **2008**, *41*, 3620–3626. (j) Ohno, K.; Morinaga, T.; Takeno, S.; Tsujii, Y.; Fukuda, T. *Macromolecules* **2007**, *40*, 9143–9150. (k) Mandal, T. K.; Fleming, M. S.; Walt, D. R. *Chem. Mater.* **2000**, *12*, 3481–3487.

(19) (a) Baskaran, D.; Mays, J. W.; Bratcher, M. S. *Angew. Chem., Int. Ed.* **2004**, *43*, 2138–2142. (b) Qin, S.; Qin, D.; Ford, W. T.; Resasco, D. E.; Herrera, J. E. *J. Am. Chem. Soc.* **2004**, *126*, 170–176. (c) Kong, H.; Gao, C.; Yan, D. *J. Am. Chem. Soc.* **2004**, *126*, 412–413.

(20) Chung, H.; Ohno, K.; Fukuda, T.; Composto, R. J. *Nano Lett.* **2005**, *5*, 1878–1882.

(21) (a) Raula, J.; Shan, J.; Nuopponen, M.; Niskanen, A.; Jiang, H.; Kauppinen, E. I.; Tenhu, H. *Langmuir* **2003**, *19*, 3499–3504. (b) Shan, J.; Nuopponen, M.; Jiang, H.; Kauppinen, E.; Tenhu, H. *Macromolecules* **2003**, *36*, 4526–4533. (c) Kizhakkedathu, J. N.; Norris-Jones, R.; Brooks, D. E. *Macromolecules* **2004**, *37*, 734–743. (d) Kim, D. J.; Kang, S. M.; Kong, B.; Kim, W.-J.; Paik, H.-J.; Choi, H.; Choi, I. S. *Macromol. Chem. Phys.* **2005**, *206*, 1941–1946. (e) Wu, T.; Zhang, Y. F.; Wang, X. F.; Liu, S. Y. *Chem. Mater.* **2008**, *20*, 101–109.

(22) (a) Li, D. J.; Jones, G. L.; Dunlap, J. R.; Hua, F. J.; Zhao, B. *Langmuir* **2006**, *22*, 3344–3351. (b) Li, D. J.; Zhao, B. *Langmuir* **2007**, *23*, 2208–2217. (c) Li, D. J.; Dunlap, J. R.; Zhao, B. *Langmuir* **2008**, *24*, 5911–5918.

(23) (a) Piech, M.; Bell, N. S. *Macromolecules* **2006**, *39*, 915–922. (b) Piech, M.; George, M. C.; Bell, N. S.; Braun, P. V. *Langmuir* **2006**, *22*, 1379–1382.

(24) Gil, E. S.; Hudson, S. M. *Prog. Polym. Sci.* **2004**, *29*, 1173–1222.

(25) Schild, H. G. *Prog. Polym. Sci.* **1992**, *17*, 163–249.

(26) Li, D. J.; Sheng, X.; Zhao, B. *J. Am. Chem. Soc.* **2005**, *127*, 6248–6256.

(27) (a) Marko, J. F.; Witten, T. A. *Phys. Rev. Lett.* **1991**, *66*, 1541–1544. (b) Marko, J. F.; Witten, T. A. *Macromolecules* **1992**, *25*, 296–307. (c) Dong, H. *J. Phys. II* **1993**, *3*, 999–1020. (d) Brown, G.; Chakrabarti, A.; Marko, J. F. *Europhys. Lett.* **1994**, *25*, 239–244.

(28) (a) Lai, P. Y. *J. Chem. Phys.* **1994**, *100*, 3351–3357. (b) Soga, K. G.; Zuckermann, M. J.; Guo, H. *Macromolecules* **1996**, *29*, 1998–2005. (c) Zhulina, E.; Balazs, A. C. *Macromolecules* **1996**, *29*, 2667–2673. (d) Müller, M. *Phys. Rev. E* **2002**, *65*, 030802. (e) Minko, S.; Müller, M.; Usov, D.; Scholl, A.; Froeck, C.; Stamm, M. *Phys. Rev. Lett.* **2002**, *88*, 035502. (f) Wenning, L.; Müller, M.; Binder, K. *Europhys. Lett.* **2005**, *71*, 639–645. (g) Wang, J.; Müller, M. *J. Phys. Chem. B* **2009**, *113*, 11384–11402.

(29) (a) Singh, C.; Pickett, G. T.; Balazs, A. C. *Macromolecules* **1996**, *29*, 7559–7570. (b) Chen, C.; Dan, N.; Dhoot, S.; Tirrell, M.; Mays, J.; Watanabe, H. *Isr. J. Chem.* **1995**, *35*, 41–47. (c) Merlitz, H.; He, G. L.; Sommer, J. U.; Wu, C. X. *Macromolecules* **2009**, *42*, 445–451. (d) Uhlmann, P.; Merlitz, H.; Sommer, J. U.; Stamm, M. *Macromol. Rapid Commun.* **2009**, *30*, 732–740.

(30) Witte and Won recently studied mixed brushes with the grafting sites mobile at interface, allowing macroscopic phase separation. This situation will not be discussed in this article. (a) Witte, K. N.; Won, Y.-Y. *Macromolecules* **2006**, *39*, 7757–7768. (b) Witte, K. N.; Won, Y.-Y. *Macromolecules* **2008**, *41*, 2735–2738.

(31) Sidorenko, A.; Minko, S.; Schenk-Meuser, K.; Duschner, H.; Stamm, M. *Langmuir* **1999**, *15*, 8349–8355.

(32) (a) Luzinov, I.; Minko, S.; Tsukruk, V. V. *Prog. Polym. Sci.* **2004**, *29*, 635–698. (b) Uhlmann, P.; Ionov, L.; Houbenov, N.; Nitschke, M.; Grundke, K.; Motornov, M.; Minko, S.; Stamm, M. *Prog. Org. Coat.* **2006**, *55*, 168–174. (c) Minko, S. *Polym. Rev.* **2006**, *46*, 397–420. (d) Luzinov, I.; Minko, S.; Tsukruk, V. V. *Soft Matter* **2008**, *4*, 714–725.

(33) Minko, S.; Usov, D.; Goreshnik, E.; Stamm, M. *Macromol. Rapid Commun.* **2001**, *22*, 206–211.

(34) Minko, S.; Müller, M.; Usov, D.; Scholl, A.; Froeck, C.; Stamm, M. *Phys. Rev. Lett.* **2002**, *88*, 035502.

(35) Motornov, M.; Minko, S.; Eichhorn, K. J.; Nitschke, M.; Simon, F.; Stamm, M. *Langmuir* **2003**, *19*, 8077–8085.

(36) Feng, J. X.; Haasch, R. T.; Dyer, D. J. *Macromolecules* **2004**, *37*, 9525–9537.

(37) Lemieux, M.; Usov, D.; Minko, S.; Stamm, M.; Shulha, H.; Tsukruk, V. V. *Macromolecules* **2003**, *36*, 7244–7255.

(38) Usov, D.; Gruzdev, V.; Nitschke, M.; Stamm, M.; Hoy, O.; Luzinov, I.; Tokarev, I.; Minko, S. *Macromolecules* **2007**, *40*, 8774–8783.

(39) Santer, S.; Kopyshev, A.; Yang, H. K.; Rühe, J. *Macromolecules* **2006**, *39*, 3056–3064.

(40) Santer, S.; Kopyshev, A.; Donges, J.; Yang, H. K.; Rühe, J. *Langmuir* **2006**, *22*, 4660–4667.

(41) Santer, S.; Rühe, J. *Polymer* **2004**, *45*, 8279–8297.

(42) Zhang, J.; Yang, Y.; Zhao, C.; Zhao, H. *J. Polym. Sci., Part A: Polym. Chem.* **2007**, *45*, 5329–5338.

(43) Minko, S.; Patil, S.; Datsyuk, V.; Simon, F.; Eichhorn, K. J.; Motornov, M.; Usov, D.; Tokarev, I.; Stamm, M. *Langmuir* **2002**, *18*, 289–296.

(44) Minko, S.; Luzinov, I.; Luchnikov, V.; Müller, M.; Patil, S.; Stamm, M. *Macromolecules* **2003**, *36*, 7268–7279.

(45) Houbenov, N.; Minko, S.; Stamm, M. *Macromolecules* **2003**, *36*, 5897–5901.

(46) Minko, S.; Müller, M.; Motornov, M.; Nitschke, M.; Grundke, K.; Stamm, M. *J. Am. Chem. Soc.* **2003**, *125*, 3896–3900.

(47) Ionov, L.; Minko, S.; Stamm, M.; Gohy, J. F.; Jerome, R.; Scholl, A. *J. Am. Chem. Soc.* **2003**, *125*, 8302–8306.

(48) Draper, J.; Luzinov, I.; Minko, S.; Tokarev, I.; Stamm, M. *Langmuir* **2004**, *20*, 4064–4075.

(49) Ionov, L.; Sidorenko, A.; Stamm, M.; Minko, S.; Zdyrko, B.; Klep, V.; Luzinov, I. *Macromolecules* **2004**, *37*, 7421–7423.

(50) Ionov, L.; Stamm, M.; Minko, S.; Hoffmann, F.; Wolff, T. *Macromol. Symp.* **2004**, *210*, 229–235.

(51) Ionov, L.; Houbenov, N.; Sidorenko, A.; Stamm, M.; Luzinov, I.; Minko, S. *Langmuir* **2004**, *20*, 9916–9919.

(52) Ionov, L.; Sidorenko, A.; Stamm, M.; Minko, S.; Zdyrko, B.; Klep, V.; Luzinov, I. *Macromolecules* **2004**, *37*, 7421–7423.

(53) Motornov, M.; Sheparovych, R.; Tokarev, I.; Roiter, Y.; Minko, S. *Langmuir* **2007**, *23*, 13–19.

(54) Mikhaylova, Y.; Ionov, L.; Rappich, J.; Gensch, M.; Esser, N.; Minko, S.; Eichhorn, K. J.; Stamm, M.; Hinrichs, K. *Anal. Chem.* **2007**, *79*, 7676–7682.

(55) Sheparovych, R.; Motornov, M.; Minko, S. *Langmuir* **2008**, *24*, 13828–13832.

(56) LeMieux, M. C.; Julthongpiput, D.; Bergman, K. N.; Cuong, P. D.; Ahn, H. S.; Lin, Y. H.; Tsukruk, V. V. *Langmuir* **2004**, *20*, 10046–10054.

(57) Wang, J.; Kara, S.; Long, T. E.; Ward, T. C. *J. Polym. Sci., Polym. Chem.* **2000**, *38*, 3742–3750.

(58) Julthongpiput, D.; Lin, Y. H.; Teng, J.; Zubarev, E. R.; Tsukruk, V. V. *Langmuir* **2003**, *19*, 7832–7836.

(59) Julthongpiput, D.; Lin, Y. H.; Teng, J.; Zubarev, E. R.; Tsukruk, V. V. *J. Am. Chem. Soc.* **2003**, *125*, 15912–15921.

(60) Wang, Y.; Zheng, J. X.; Brittain, W. J.; Cheng, S. Z. D. *J. Polym. Sci., Part A: Polym. Chem.* **2006**, *44*, 5608–5617.

(61) Zhao, B. *Polymer* **2003**, *44*, 4079–4083.

(62) Zhao, B. *Langmuir* **2004**, *20*, 11748–11755.

(63) Zhao, B.; He, T. *Macromolecules* **2003**, *36*, 8599–8602.

(64) Zhao, B.; Haasch, R. T.; MacLaren, S. *J. Am. Chem. Soc.* **2004**, *126*, 6124–6134.

(65) Zhao, B.; Haasch, R. T.; MacLaren, S. *Polymer* **2004**, *45*, 7979–7988.

(66) Lin, Y. H.; Teng, J.; Zubarev, E. R.; Shulha, H.; Tsukruk, V. V. *Nano Lett.* **2005**, *5*, 491–495.

(67) Ionov, L.; Houbenov, N.; Sidorenko, A.; Stamm, M.; Minko, S. *Adv. Funct. Mater.* **2006**, *16*, 1153–1160.

(68) Zdyrko, B.; Klep, V.; Li, X. W.; Kang, Q.; Minko, S.; Wen, X. J.; Luzinov, I. *Mater. Sci. Eng., C* **2009**, *29*, 680–684.

(69) Motornov, M.; Sheparovych, R.; Katz, E.; Minko, S. *ACS Nano* **2008**, *2*, 41–52.
(70) He, T.; Li, D. J.; Sheng, X.; Zhao, B. *Macromolecules* **2004**, *37*, 3128–3135.
(71) In principle, one can use a soft, planar substrate to prepare mixed brushes for microtoming.
(72) It should be noted here that polymeric micelles with mixed chains in the corona layer can be viewed as mixed brush-grafted particles, where the core is a "soft" polymeric particle. Nanoscale phase separation has been observed in this type of block copolymer micelles. (a) Gohy, J.-F.; Khousakoun, E.; Willet, N.; Varshney, S. K.; Jérôme, R. *Macromol. Rapid Commun.* **2004**, *25*, 1536–1539. (b) Hu, J.; Liu, G. *Macromolecules* **2005**, *38*, 8058–8065. (c) Chen, K.; Liang, D.; Tian, J.; Shi, L.; Zhao, H. *J. Phys. Chem. B* **2008**, *112*, 12612–12617. These micelles are not discussed in this article since here we focus on mixed brushes grafted on a "hard" inorganic core.
(73) Roan, J.-R. *Phys. Rev. Lett.* **2006**, *96*, 248301.
(74) Zhao, B.; Zhu, L. *J. Am. Chem. Soc.* **2006**, *128*, 4574–4575.
(75) Zhu, L.; Zhao, B. *J. Phys. Chem. B* **2008**, *112*, 11529–11536.
(76) Motornov, M.; Sheparovych, R.; Lupitskyy, R.; MacWilliams, E.; Minko, S. *J. Colloid Interface Sci.* **2007**, *310*, 481–488.
(77) Motornov, M.; Sheparovych, R.; Lupitskyy, R.; MacWilliams, E.; Minko, S. *Adv. Mater.* **2008**, *20*, 200–205.
(78) Cheng, J.; He, J.; Li, C.; Yang, Y. *Chem. Mater.* **2008**, *20*, 4224–4230.
(79) Shan, J.; Nuopponen, M.; Jiang, H.; Viitala, T.; Kauppinen, E.; Kontturi, K.; Tenhu, H. *Macromolecules* **2005**, *38*, 2918–2926.
(80) Shan, J.; Chen, J.; Nuopponen, M.; Viitala, T.; Jiang, H.; Peltonen, J.; Kauppinen, E.; Tenhu, H. *Langmuir* **2006**, *22*, 794–801.
(81) Shan, J.; Tenhu, H. *Chem. Commun.* **2007**, 4580–4598.
(82) Zubarev, E. R.; Xu, J.; Sayyad, A.; Gibson, J. D. *J. Am. Chem. Soc.* **2006**, *128*, 4958–4959.
(83) Zubrev, E. R.; Xu, J.; Sayyad, A.; Gibson, J. D. *J. Am. Chem. Soc.* **2006**, *128*, 15098–15099.
(84) Genson, K. L.; Holzmueller, J.; Jiang, C.; Xu, J.; Gibson, J. D.; Zubarev, E. R.; Tsukruk, V. V. *Langmuir* **2006**, *22*, 7011–7015.
(85) Guo, Y.; Moffitt, M. G. *Macromolecules* **2007**, *40*, 5868–5878.
(86) Guo, Y.; Moffitt, M. G. *Chem. Mater.* **2007**, *19*, 6581–6587.
(87) Boyer, C.; Whittaker, M. R.; Luzon, M.; Davis, T. P. *Macromolecules* **2009**, *42*, 6917–6926.
(88) Chiu, J. J.; Kim, B. J.; Kramer, E. J.; Pine, D. J. *J. Am. Chem. Soc.* **2005**, *127*, 5036–5037.
(89) Kim, B. J.; Fredrickson, G. H.; Hawker, C. J.; Kramer, E. J. *Langmuir* **2007**, *23*, 7804–7809.
(90) Kim, B. J.; Bang, J.; Hawker, C. J.; Chiu, J. J.; Pine, D. J.; Jang, S. G.; Yang, S.-M.; Kramer, E. J. *Langmuir* **2007**, *23*, 12693–12703.
(91) Hamley, I. W. *The Physics of Block Copolymers*; Oxford University Press: Oxford, 1998.
(92) Hamley, I. W. *Block Copolymers in Solution: Fundamentals and Applications*; John Wiley & Sons: Chichester, 2005.
(93) Santer, S.; Kopyshev, A.; Donges, J.; Rühe, J.; Jiang, X. G.; Zhao, B.; Muller, M. *Langmuir* **2007**, *23*, 279–285.
(94) Chen, W. Y.; Zheng, J. X.; Cheng, S. Z. D.; Li, C. Y.; Huang, P.; Zhu, L.; Xiong, H. M.; Ge, Q.; Guo, Y.; Quirk, R. P.; Lotz, B.; Deng, L. F.; Wu, C.; Thomas, E. L. *Phys. Rev. Lett.* **2004**, *93*, 028301.
(95) (a) Zhao, B.; Brittain, W. J. *J. Am. Chem. Soc.* **1999**, *121*, 3557–3558. (b) Zhao, B.; Brittain, W. J.; Zhou, W.; Cheng, S. Z. D. *J. Am. Chem. Soc.* **2000**, *122*, 2407–2408.
(96) (a) Han, S.; Hagiwara, M.; Ishizone, T. *Macromolecules* **2003**, *36*, 8312–8319. (b) Zhao, B.; Li, D. J.; Hua, F. J.; Green, D. R. *Macromolecules* **2005**, *38*, 9509–9517. (c) Hua, F. J.; Jiang, X. G.; Li, D. J.; Zhao, B. *J. Polym. Sci., Part A: Polym. Chem.* **2006**, *44*, 2454–2467. (d) Hua, F. J.; Jiang, X. G.; Zhao, B. *Macromolecules* **2006**, *39*, 3476–3479. (e) Lutz, J.-F.; Hoth, A. *Macromolecules* **2006**, *39*, 893–896. (f) Jiang, X. G.; Zhao, B. *J. Polym. Sci., Part A: Polym. Chem.* **2007**, *45*, 3707–3721. (g) Jiang, X. G.; Lavender, C. A.; Woodcock, J. W.; Zhao, B. *Macromolecules* **2008**, *41*, 2632–2643. (h) Jiang, X. G.; Zhao, B. *Macromolecules* **2008**, *41*, 9366–9375. (i) Jiang, X. G.; Jin, S.; Zhong, Q. X.; Dadmun, M. D.; Zhao, B. *Macromolecules* **2009**, *42*, 8468–8476. (j) O'Lenick, T. G.; Jiang, X. M.; Zhao, B. *Polymer* **2009**, *50*, 4363–4371.
(97) Manoharan, V. N.; Elsesser, M. T.; Pine, D. J. *Science* **2003**, *301*, 483.
(98) Zhang, Z. L.; Glotzer, S. C. *Nano Lett.* **2004**, *4*, 1407–1413.
(99) Jackson, A. M.; Myerson, J. W.; Stellacci, F. *Nat. Mater.* **2004**, *3*, 330–336.
(100) Helms, B.; Guillaudeu, S. J.; Xie, Y.; McMurdo, M.; Hawker, C. J.; Fréchet, J. M. J. *Angew. Chem., Int. Ed.* **2005**, *44*, 6384–6387.
(101) Voit, B. *Angew. Chem., Int. Ed.* **2006**, *45*, 4238–4240.
(102) Dong, H.; Marko, J. F.; Witten, T. A. *Macromolecules* **1994**, *27*, 6428–6442.